AD-A173 085 DETERMINING AND MODELING THE RESPONSE OF YTTERBIUM PIEZORESISTANCE TRANSDUCERS(U) WASHINGTON STATE UNIV PULLMAN SHOCK DYNAMICS LAB Y M GUPTA MAY 86 1/1

UNCLASSIFIED AFOSR-TR-86-0864 AFOSR-82-0132 F/G 9/1 NL

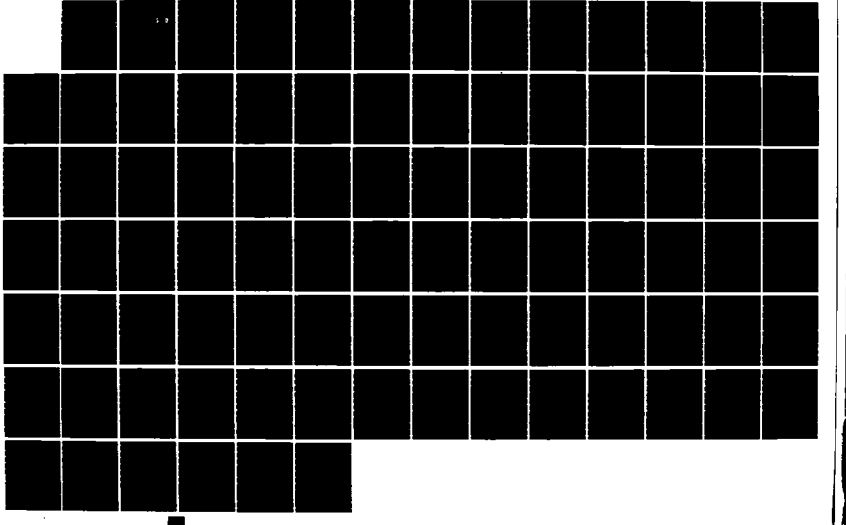

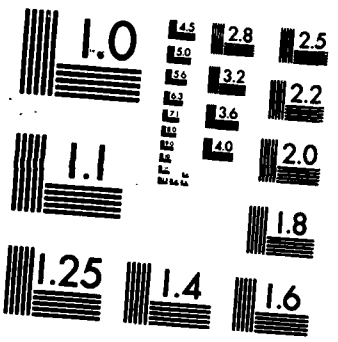

DETERMINING AND MODELING THE RESPONSE OF YTTERBIUM PIEZORESISTANCE TRANSDUCERS

Principal Investigator
Y.M. Gupta
Shock Dynamics Laboratory
Department of Physics
Washington State University
Pullman, WA 99164-2814

FINAL REPORT

4/82 - 3/86

Approved for public release;
distribution unlimited.

WORK SPONSORED BY THE AIR FORCE OFFICE OF SCIENTIFIC RESEARCH

Under Grant No. 82-0132

May 1986

WSU Project No. 2464-0110

UNCLASSIFIED
SECURITY CLASSIFICATION OF THIS PAGE

AD-A173 085

REPORT DOCUMENTATION PAGE

1a. REPORT SECURITY CLASSIFICATION: UNCLASSIFIED	1b. RESTRICTIVE MARKINGS
2a. SECURITY CLASSIFICATION AUTHORITY	3. DISTRIBUTION/AVAILABILITY OF REPORT: Approved for Public Release; Distribution Unlimited.
2b. DECLASSIFICATION/DOWNGRADING SCHEDULE	
4. PERFORMING ORGANIZATION REPORT NUMBER(S)	5. MONITORING ORGANIZATION REPORT NUMBER(S): AFOSR-TR- 86-0884
6a. NAME OF PERFORMING ORGANIZATION: WASHINGTON STATE UNIVERSITY DEPARTMENT OF PHYSICS,SDL; 6b. OFFICE SYMBOL (If applicable)	7a. NAME OF MONITORING ORGANIZATION: AFOSR
6c. ADDRESS (City, State and ZIP Code): PULLMAN, WA 99164-2814	7b. ADDRESS (City, State and ZIP Code): Same as 8c
8a. NAME OF FUNDING/SPONSORING ORGANIZATION: AIR FORCE OFFICE OF SCIENTIFIC RESEARCH; 8b. OFFICE SYMBOL (If applicable): AFOSR/NA	9. PROCUREMENT INSTRUMENT IDENTIFICATION NUMBER: Grant No. 82-0132
8c. ADDRESS (City, State and ZIP Code): BOLLING AFB, DC 20332	10. SOURCE OF FUNDING NOS.

PROGRAM ELEMENT NO.	PROJECT NO.	TASK NO.	WORK UNIT NO.
61102F	2302	C1	

11. TITLE (Include Security Classification): DETERMINING AND MODELING THE RESPONSE OF YTTERBIUM PIEZORESISTANCE TRANSDUCERS (UNCLASSIFIED)

12. PERSONAL AUTHOR(S): GUPTA, YOGENDRA M.

13a. TYPE OF REPORT	13b. TIME COVERED	14. DATE OF REPORT (Yr., Mo., Day)	15. PAGE COUNT
FINAL REPORT	FROM 4/82 TO 3/86	May 1986	83

16. SUPPLEMENTARY NOTATION

17. COSATI CODES		
FIELD	GROUP	SUB. GR.

18. SUBJECT TERMS (Continue on reverse if necessary and identify by block number): PIEZORESISTANCE; HIGH STRESSES; SHOCK WAVE; HIGH STRAIN-RATE; YTTERBIUM

19. ABSTRACT (Continue on reverse if necessary and identify by block number)

The objectives and results of a research effort undertaken to understand the response of ytterbium stress transducers under shock loading are presented. Plate impact experiments, using matrix materials that covered a wide range of mechanical impedances, were performed to determine the gauge response under well characterized conditions. Experiments were designed to conform closely to the requirements of the theoretical analysis. Residual resistance measurements, loading rate effects, and effect of matrix property variations were examined in detail. Quasi-static experimental methods and related analysis were developed to determine the complete set of electro-mechanical constants for the foils of interest. The phenomenological model developed earlier was extended to include strain-hardening in a consistent manner. The model predictions, using the appropriate material constants, agreed very well with the shock wave measurements. Using the analytic model a good understanding of ytterbium stress transducers was achieved.

20. DISTRIBUTION/AVAILABILITY OF ABSTRACT	21. ABSTRACT SECURITY CLASSIFICATION
UNCLASSIFIED/UNLIMITED ☒ SAME AS RPT. ☐ DTIC USERS ☐	UNCLASSIFIED

22a. NAME OF RESPONSIBLE INDIVIDUAL	22b. TELEPHONE NUMBER (Include Area Code)	22c. OFFICE SYMBOL
Lt. Col. Lawrence D. Hokanson	202/767-4935	AFOSR/NA

DD FORM 1473, 83 APR EDITION OF 1 JAN 73 IS OBSOLETE.

ACKNOWLEDGMENTS

It is a pleasure to acknowledge the hard work and dedication of the various individuals involved in this effort. Drs. S.C. Gupta, D.Y. Chen, and N.S. Brar are sincerely thanked for their many contributions to the different phases of this research project. The specific problems that they have contributed to are listed in Section III. The superior efforts of Mr. Martin Williams and Mr. Jerry Thompson were a major factor in the success of the experimental program. These individuals are gratefully acknowledged for their work.

Discussions with Mr. D.D. Keough (SRI International), Professor G.E. Duvall (Washington State University), Dr. Marvin Ito (CRT) were helpful during the course of this work.

Table of Contents

I. INTRODUCTION

A. Background

The need to obtain time-resolved stress measurements is central to both fundamental studies and applications involving dynamic loading. The development of constitutive relations at high loading rates is dependent upon appropriate material property measurements which in turn depend upon accurate measurements of the different components of the stress tensor in the medium of interest. There are two types of stress transducers available for time-resolved stress measurements at stresses exceeding a kilobar (0.1 GPa)[1]: piezoelectric crystals and piezoresistance foils. Piezoelectric gauges provide higher time resolution and are simpler to use. However, their stress and time ranges are quite limited. In contrast, piezoresistance foil gauges can be used over a wide range of stresses (1 MPa - 100 GPa) and times (10 ns - static loading). Because of their adaptability and survivability, piezoresistance gauges are used widely in applications involving dynamic loading. Despite the wide usage, a detailed understanding and interpretation of the gauge response is not straightforward because of several noteworthy problems: lack of a detailed understanding of the gauge response particularly hysteresis effects; difficulty in using gauge calibration data for loading conditions that deviate from the loading conditions of the calibration experiments; variations in the gauge material, and gauge element configurations and/or gauge package designs.

Because of the importance of piezoresistance measurements to many experimental situations, a preliminary research effort (sponsored by DNA) was started in 1979 to determine the possibility of achieving a detailed understanding of piezoresistance transducers. This effort, completed successfully in 1980, has been reported in a DNA report[2] and in journal articles.[3,4] A discussion of the work prior to 1979 and some of the difficulties associated with these studies is presented in References 2 and 3. An important achievement of the DNA sponsored effort was the development of a theoretical framework to analyze and interpret piezoresistance gauge measurements. The analytic developments consisted of a phenomenological electromechanical model for piezoresistance and an elastic-plastic inclusion analysis based on an extension of Eshelby's work.[5] The combination of these developments explained, in principle, many aspects of piezoresistance gauges and suggested that on the basis of this theoretical framework we may be able to achieve a detailed understanding of piezoresistance gauges. In addition, the theory predicted several interesting results that had not been observed experimentally. However, no quantitative evaluations of the theoretical model could be undertaken in 1980-81 because of a lack of needed material parameters for the gauge foils, relevant experimental data, and

the need to incorporate strain-hardening in the theoretical analysis. This last item involved a non-trivial extension of the theoretical analysis.

Although a good start had been made in the preliminary effort, a longer term research program with strong emphasis on interaction between theory and experiment was needed to develop a comprehensive understanding of piezoresistance gauges. Such an effort was started, under AFOSR sponsorship, on ytterbium transducers because of their applicability at low stresses (0.1 kbar - 30 kbar).* We have chosen to study ytterbium because it is nearly two orders of magnitude more sensitive than manganin and is ideally suited for use at low stresses. The upper limit of ytterbium is approximately 30-40 kbar because of the FCC→BCC phase transition that occurs in the 35-40 kbar range in static high pressure studies. The useful range of ytterbium is well suited for Air Force applications and this material is now the most popular sensing element in flat pack gauges used in fielding applications. Hence, a detailed and fundamental understanding of the transducer material is very desirable. The objectives and approach relevant to the present work are presented next.

B. Objectives and Approach

The overall goal of our work was to develop an in-depth understanding of ytterbium piezoresistance gauges to enable accurate stress measurements in materials and in applications of interest by building on the theoretical work described in Reference 2. Specifically, we hoped to complete the following tasks:

1. Extend the theoretical work to incorporate strain-hardening. This extension is necessary to understand and model the observed gauge hysteresis.
2. Design and perform a set of base-line dynamic experiments that conform closely to the requirements of the theoretical analyses. These data could then be used to check the theoretical calculations.
3. Development of a quasi-static experimental method and analysis to measure the material constants that appear in the theoretical relations. This development is necessary to address the problem of material variability.
4. Supplement the base-line dynamic experiments with other dynamic experiments to determine the effects of matrix variation and loading rates on the piezoresistance response.

---

* A complementary effort at higher stresses using manganin transducers and fluid encapsulated gauges was started under DNA sponsorship.

5. Perform detailed analyses to model the gauge hysteresis observations and the observed effects of matrix variation on piezoresistance measurements.

6. Examine the feasibility of measuring the complete stress tensor, that is --components perpendicular to the direction of the shock front. This is a problem of long standing in shock wave studies and is central to the use of shock wave methods for developing high strain-rate constitutive models.

To achieve these objectives, we chose to perform well-defined, gas-gun experiments and related analyses. In these experiments, the piezoresistance gauge is subjected to a nearly square stress-pulse of approximately 1-2 μs duration. This is achieved by impacting a thin (3-5 mm thickness) flyer plate of a well characterized material on target plates of the same material. By varying the impact velocity and the impacting materials, the pulse amplitude can be controlled. The pulse duration is determined by the flyer plate thickness. Gauge foils are cut into Π-shaped elements and emplaced into grooves machined into the matrix materials. Care is taken to ensure that the gauge elements and the grooves are nearly identical in size and that a minimum of glue bond is used in sample assembly. Further details of the experimental method may be seen in Reference 6 or in Appendix 2 of this report.

The emphasis was on developing a detailed understanding of piezoresistance measurements that would be pertinent to a broad range of applications. This approach necessitated the use of matrix materials (PMMA, Fused Silica, polycrystalline Al_2O_3) that were well characterized under shock loading and covered a wide range of mechanical impedances. Gauge emplacement and sample assembly procedures, though more complicated than previous studies, were designed to conform closely to the requirements of the theoretical analysis. For example, in our work the piezoresistance foils are themselves the inclusions as opposed to the use of a gauge package; it is nearly impossible to analyze the gauge package quantitatively without making assumptions about the constitutive properties of the gauge package components.

We believe that a detailed understanding of piezoresistance measurements under near-ideal conditions (direct problem) is a necessary step towards the development of a gauge package designed to measure the stress components of interest under dynamic loading conditions. In the latter problem, one is inverting the resistance change data to obtain the stress component of interest.

II. RESULTS AND DISCUSSION

A summary of the experimental results and related analyses pertinent to the tasks outlined in the last section is presented here. Figures pertinent to work that has already been published are not reproduced here and may be seen in the literature. Important figures from manuscripts that have not been published are presented in this section. Work described in Sections II.A, B, E, and G has already been published. Manuscripts describing work in Sections II.C, and D have been submitted and are attached as Appendices to this report. The manuscript describing work in Section II.F is currently under preparation and will be submitted shortly.

A. Dynamic Experiments in PMMA[6]

The experimental technique developed by Gupta et al.[7] was refined to obtain resistance change measurements in ytterbium foils shocked to 2.5 GPa (25 kbar) in a PMMA matrix. Gauges were oriented parallel and perpendicular to the shock front to examine the feasibility of specifying the complete stress tensor in the matrix material. The results of this work are as follows:

1. Data for the two foil orientations were obtained between 0.1 to 2.5 GPa. These results supported the phenomenological model described in Ref. 3. In particular, the crossover in resistance change values for the two orientations, predicted at low stresses by the model, was demonstrated.
2. Residual resistance-change data were obtained over the entire stress range. These data showed that the results could be broken into three distinct regions: the residual resistance-change was zero below the stress threshold for inelastic deformation in ytterbium; the near parabolic shape of the residual resistance-change versus stress curve beyond the stress threshold for inelastic deformation in ytterbium; a rapid increase in the residual resistance-change near the onset of inelastic deformation in PMMA followed by constant value.
3. Our results suggested that the use of ytterbium foils be restricted to stresses below 20 kbar in the matrix material. Beyond this value, the ytterbium response appears to be dependent on the properties of the encapsulating material. This stress value may be the precursor to the FCC→BCC transition observed in static high pressure studies.
4. The resistance change measurements for the two orientations demonstrate that PMMA maintains significant strength to 25 kbar. This result contradicts earlier inferences of strength loss in PMMA.

B. Quasi-Static Experiments to Determine Electro-Mechanical Constants[8]

A problem of long standing in using piezoresistance gauges in shock wave studies is the batch-to-batch material variability and variations in gauge design. This has led to a number of empirical studies designed to calibrate a particular batch of foils or a particular gauge design. This approach is not only time consuming and expensive but is of limited applicability to other batches or gauge designs. Furthermore, results of such studies cannot be related to more general loading conditions. What is needed is an experimental method that permits evaluation of the fundamental electro-mechanical constants that occur in the relations linking resistivity changes to mechanical deformation in the foils. In addition, the experimental method and analysis have to be relatively simple so that foils from different batches can be efficiently characterized.

In this work, experimental techniques and related analyses were developed and used to measure the mechanical and piezoresistive coefficients of the foils of interest. These developments, in conjunction with hydrostatic measurements, provide a comprehensive characterization of the electro-mechanical constants needed to characterize piezoresistance foils. The relative ease of the method mitigates problems of material reproducibility and minimizes the number of shock wave experiments needed to calibrate the gauge response. Hence, this experimental development has considerable practical significance.

The quasi-static results supported an important assumption in the phenomenological model: the onset of mechanical yield coincides with the permanent change in resistivity of the foils that were examined. The analytic developments in this work provided a simple yet realistic description of resistance effects related to mechanical deformation. This work, with relatively straightforward extension, can be used to measure both in-material stresses and strains in quasi-static applications.[8]

C. Incorporation of Strain-Hardening Into the Phenomenological Model (Appendix 1)

In the initial development by Gupta,[4] the need for an elastic-plastic-strain hardening description for the foils was recognized and some related theoretical developments were presented. However, the inclusion analysis was limited to an elastic-perfectly plastic inclusion because of a lack of experimental data on the appropriate material properties of the inclusion (see Section IV.B of Reference 4). Results presented in References 6 and 8, and summarized above demonstrate the need for incorporating strain-hardening into the analysis and also provide the needed material property data. In this work, the phenomenological model was extended to incorporate strain-hardening and then applied to the results summarized above in Section II.A.

The essential elements of Eshelby's analysis for an elastic, ellipsoidal inclusion[5] can be extended to an inelastic inclusion as[4]

$$\sigma = H'' \cdot \epsilon \tag{1}$$

$$\epsilon = \epsilon^C + \epsilon^A \tag{2}$$

$$\epsilon^C = S \cdot \epsilon^T \tag{3}$$

and

$$H'' \cdot (\epsilon^C + \epsilon^A) = H \cdot (\epsilon^C + \epsilon^A - \epsilon^T) \tag{4}$$

where σ = stress in the inclusion, ϵ = strain in the inclusion, ϵ^A = applied matrix strain, ϵ^T = stress free transformation strain, ϵ^C = constrained strain, S = tensor that depends on the Poisson's ratio of the matrix and shape of the inclusion, H = modulus tensor of the elastic matrix, H'' = modulus tensor of the inelastic inclusion. The main task in the present work was to obtain H'' for a strain-hardening inclusion.

The usual elements of plasticity theory were used with the yield surface expressed as

$$f = \sqrt{J'_2} - Y\ M\gamma_p = 0 \tag{5}$$

where M = strain hardening coefficient and the other symbols have the usual definition.[8] Using the results derived in Section II of Appendix 1, the summation index notation can be used to write:

$$d\sigma_{ij} = \left(K - \frac{2G}{3}\right) d\epsilon_{ll}\delta_{ij} + 2Gd\epsilon_{ij} - \frac{2G^2\sigma'_{mn}\sigma'_{ij}}{(2G + M)J'_2} d\epsilon'_{mn} \tag{6}$$

where K = bulk modulus, G = shear modulus, and the primed quantities represent deviators. This equation can be used to construct the H'' modulus tensor.

Using the developments in this work, the residual resistance change versus stress data obtained in Reference 6 were analyzed to obtain the electrical-strain-hardening function, η, as a function of plastic strain, γ_p in Figure 1. The product of η and γ_p represents the plastic strain contribution to resistivity changes.

The curve in Figure 1 along with the model are then used to calculate the resistance change versus peak longitudinal matrix stress shown in Figure 2. Up to 7.8 kbar, the PMMA constitutive response is accurately known and results for both orientations can be calculated. Beyond 7.8 kbar, the PMMA response is inelastic and the lateral gauge response cannot be calculated. The longitudinal stress in the PMMA matrix is well known and using the continuity of longitudinal stress in the PMMA and the ytterbium, we can calculate the longitudinal gauge response with reasonable

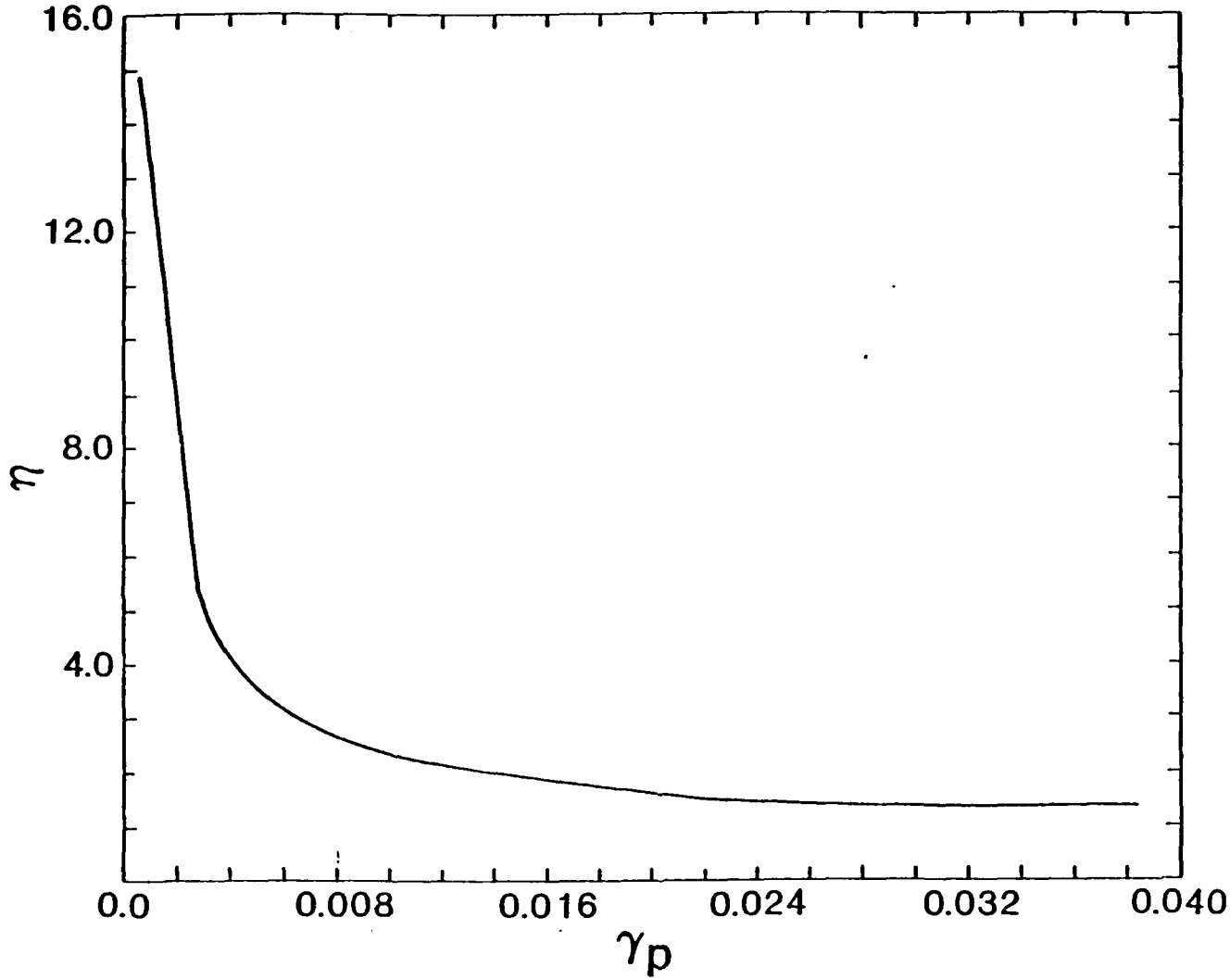

Figure 1: Calculated value of the electrical-strain-hardening function, η, as a function of plastic strain. The product of these quantities represents the contribution of plastic deformation to the resistivity change.

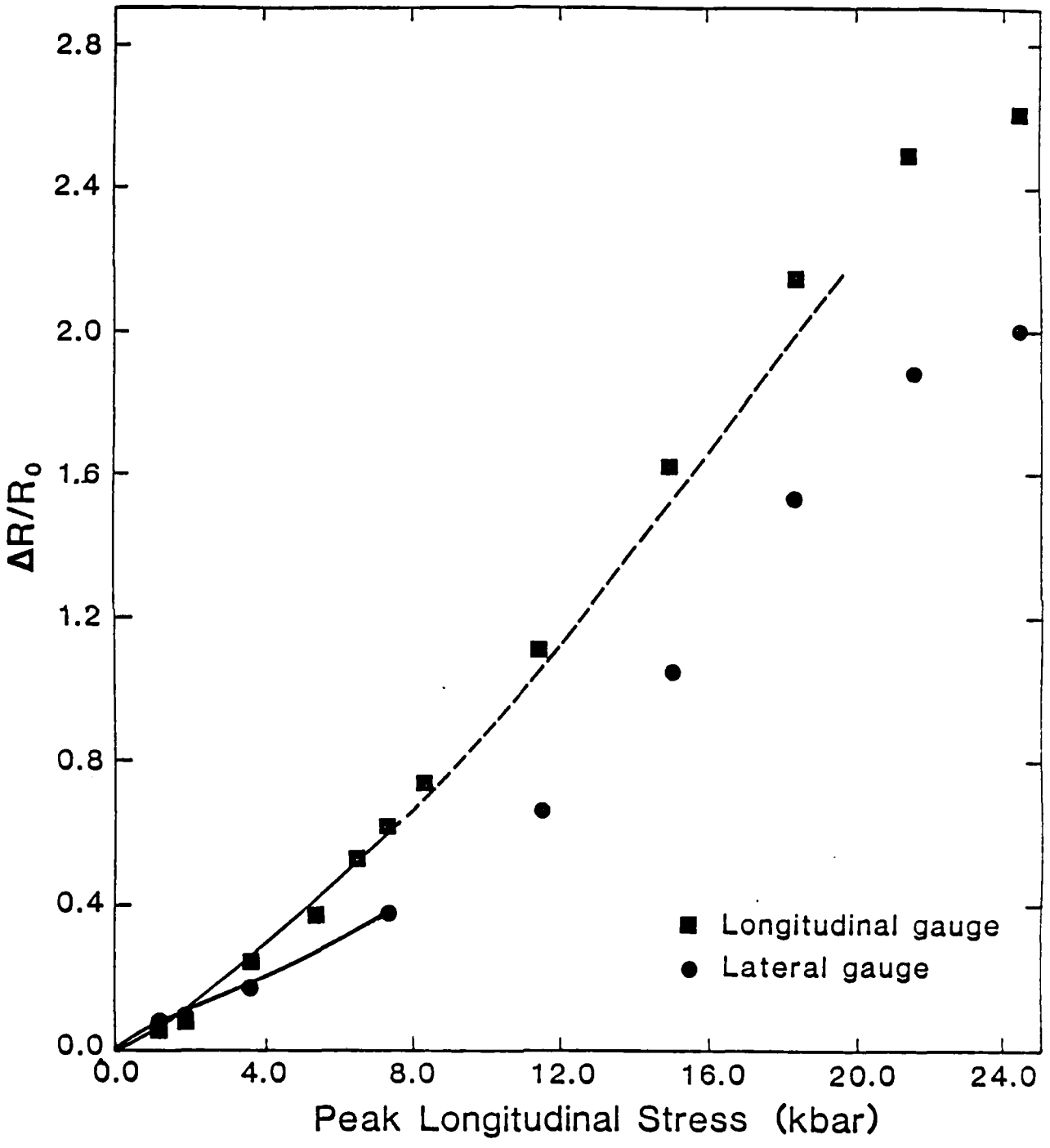

Figure 2: Measured and calculated values of the resistance change for the two gauge orientations as a function of matrix longitudinal stress. The calculated results are shown as a broken line beyond the onset of inelastic deformation in PMMA.

accuracy. Over the range which we can calculate, the model predictions are in good agreement with the experimental results.

The developments indicated here have also been successful in providing a qualitative description of the residual resistance change data observed over the entire stress range of the experiments.

D. Effect of Matrix Properties on Gauge Response

The relationship between the response of piezoresistance gauges and the properties of the matrix materials encapsulating these gauges is a question that had not been addressed satisfactorily in earlier studies. Keough and Wong[10] examined this problem for manganin but the results were not entirely conclusive.

We performed a series of experiments in which the response of ytterbium gauges was examined using two materials (polycrystalline Al_2O_3 and PMMA) with very different mechanical impedances. Two experimental configurations were employed: PMMA impactor and a polycrystalline Al_2O_3 sample; polycrystalline Al_2O_3 impactor and a PMMA sample. The use of these configurations ensures that the peak stress is identical in the samples for the two experiments. We chose a peak stress of 2.56 GPa (25.6 kbar).

The experimental results showed significant differences both in the structure of the wave-form and the steady state resistance change value. The ytterbium in PMMA gave a resistance change value of 2.6 while the ytterbium in Al_2O_3 gave a resistance change value of 1.1. This latter value was in good agreement with our model predictions. Essentially, the results can be understood as follows: the ytterbium foil impedance is much lower than the Al_2O_3 and the structure in the wave profile is the foil "ringing" to equilibrium. Once the equilibrium is nearly attained, the gauge response can be calculated by our inclusion analysis. In the steady state, the gauge shows a lower value because there is not a continuity of longitudinal stress between the gauge and the matrix. The inclusion having a lower mechanical impedance than the matrix does not support the matrix stresses and there occurs the phenomenon of "bridging." The matrix around the gauge supports much of the load.

These experimental observations and their interpretation in terms of our phenomenological model have been extremely helpful in understanding the response of piezoresistance gauges. This information is expected to be valuable in the design of gauge packages for dynamic loading applications.

E. Piezoresistance Response of Different Batches of Ytterbium Foils[11]

An important difficulty in using piezoresistance gauges is the lack of reproducibility in the piezoresistance response from different batches of foils. This difficulty has led to a number of empirical calibrations to quantify the response of a particular batch of foils and/or a particular gauge configuration. As an extension of the work reported in Section II.B, designed to mitigate the problem of batch to batch reproducibility, we undertook an investigation with the following objectives: to confirm the correlation between quasi-static and dynamic experiments reported earlier (Section II.C) by examining a different batch of ytterbium foils; to correlate the shock wave response of different batches using our analytic model.

Dynamic and quasi-static measurements similar to those reported in References 6 and 8, respectively, were performed on a new batch of ytterbium foils. The quasi-static results showed almost identical values of piezoresistive constants but large differences in the mechanical properties. The shock wave results showed the results from the present work to be close to the previous work.[6] However, the present results were consistently lower by a few percent over the range of stresses (1 - 20 kbar) examined in the present work. Using the material properties measured for the present batch of foils, the model predictions agreed very well with our measurements and provided a quantitative explanation of the lower values observed for the second batch of foils.

The agreement between the theory and the experiments for both batches confirms the overall validity of our approach and suggests that the quasi-static experiments can be used to characterize the dynamic response of the foils. The present results provide a method for using piezoresistance foils from different batches in a consistent manner.

F. Response of Ytterbium Foils Shocked to 40 kbar in an Elastic Matrix

This particular investigation had the following objectives: to ascertain the effects of loading rate, if any, on the gauge response; to measure and quantitatively analyze the response of ytterbium gauges over the stress range of its applicability (to 40 kbar) by performing experiments in a well characterized elastic matrix (fused silica); to develop a detailed understanding of the residual resistance over the entire stress range of interest; and to compare the results with the earlier results determined for a PMMA matrix.

The experimental results for peak resistance change and residual resistance change along with the calculations are shown in Figures 3 and 4, respectively. The two sets of gauges, G1 and G2, were loaded to the same stress but at different loading rates. The results shown in Figure 3

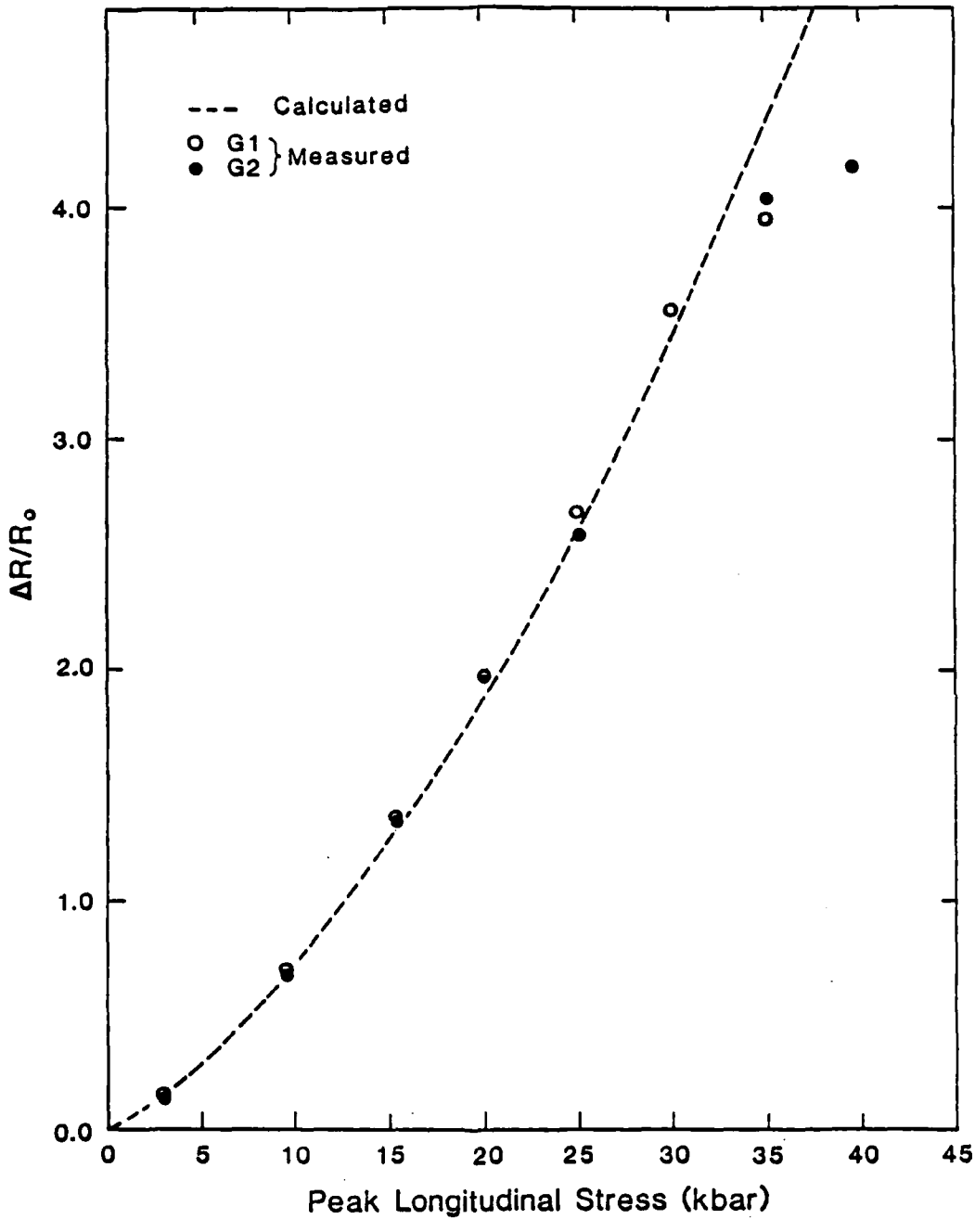

Figure 3: Measured and calculated values of peak resistance change values as a function of peak longitudinal stress in the fused silica matrix.

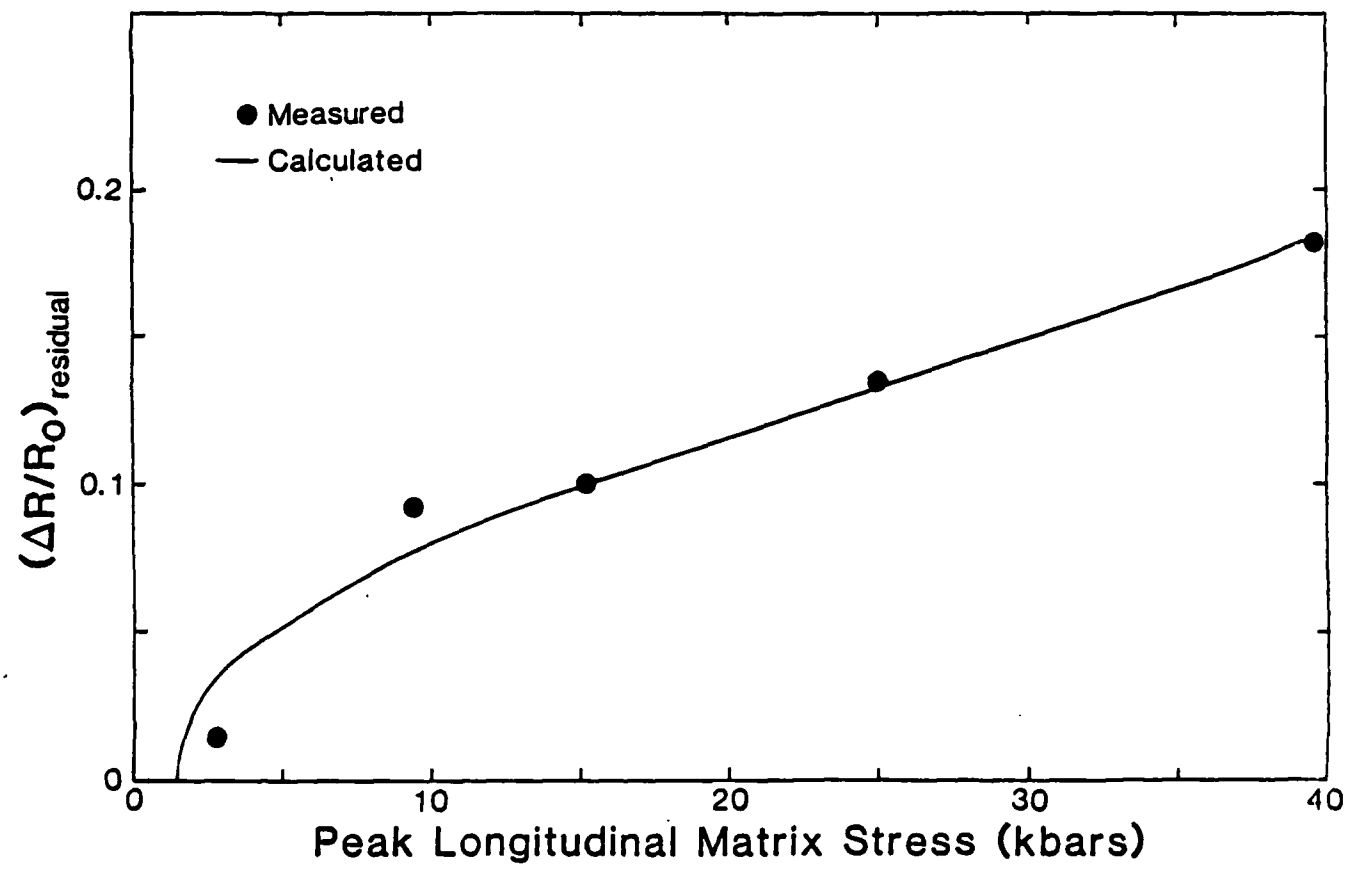

Figure 4: Measured and calculated values of residual resistance change as a function of peak longitudinal stress in the fused silica matrix.

demonstrate good agreement with the model calculations to a peak stress of 30 kbar. In addition, these results show that the gauge response is not influenced by an order of magnitude change in the loading rate (10^3 kbar - 10^4 kbar/μs). Beyond 30 kbar, the experimental results are lower because of the onset of the pressure induced FCC→BCC transition in ytterbium. This change in the slope beyond 30 kbar is very similar to that observed beyond 20 kbar in the PMMA matrix and suggests that the transition is beginning at a lower matrix stress in the PMMA matrix. The results at 45 kbar, not shown here, demonstrate clearly the phase transition observed in the material.

The residual resistance data demonstrate good overall agreement with the model predictions and demonstrate the following specific features: a threshold matrix stress for the onset of residual resistance change in ytterbium foils and a near-parabolic increase as expected from the calculations. The dominant contribution to the residual resistance is from residual stresses and strains in the foils due to plastic deformation of the foils. The matrix is elastic and away from the gauge it has zero residual stress and strains upon unloading. The point defect contributions due to plastic deformation in ytterbium contribute but are not the dominant factor.

The curve in Figure 4 is in marked contrast to that observed for the PMMA matrix (see Figure 6 of Reference 6). The residual resistance change data in PMMA show a rapid increase around 7-8 kbar which coincides with the onset of inelastic deformation in the PMMA matrix. The combination of our results for the PMMA and the fused silica matrix demonstrate the ability to use these gauges to measure residual stresses and strains in materials of interest.

The present results have provided a quantitative understanding of residual resistance (or gauge hysteresis) which has been a problem of long standing in the field of shock response of piezoresistance gauges. The ability to model the results quantitatively provides a method to account for gauge hysteresis in an experimental measurement where multiple wave structure is observed.

G. Specification of the Complete Stress Tensor in the Shocked State

The inability to measure lateral stresses in shock wave uniaxial strain experiments is a serious limitation in these experiments. Without a complete specification of the stress tensor, a good understanding of the material response of shocked solids is not possible. Previous work and some of the difficulties associated with the use of piezoresistance gauges for lateral measurements have been reviewed by Gupta et al.[7]

The basis for using piezoresistance gauges for lateral measurements is the idea that the gauge output can be uniquely related to the matrix stress component normal to the gauge foil surface (see

Figures 1 and 3 in Reference 6). The cross-over shown in Figure 5 of Reference 6 shows that this assumption is not always valid and considerable care needs to be exercised in interpreting the results. The main difficulty in the interpretation of lateral gauges is the lack of independent corroboration. The governing equations for uniaxial strain do not contain lateral stress terms and, therefore, the measurement of particle velocity is not useful for this problem.

The results of our PMMA work[6] based on the differences in the longitudinal and lateral gauge data indicate a significant strength in PMMA. However, it is not possible to quantify this strength because the methods to analyze the lateral gauge data are not well established. One can calculate the lateral gauge output in an elastic matrix as was done in our work summarized in Section II.C (see Figure 2). The good agreement observed in Figure 2 is encouraging and lends confidence to our approach. However, the calculations cannot be extended directly to an inelastic matrix without knowing the matrix constitutive properties. Because of the many inherent difficulties associated in analyzing lateral gauge data, an iterative approach to this problem was outlined in Reference 6.

The present work has been valuable in demonstrating the possibility of inferring lateral stresses in the matrix from lateral gauge data. However, there is not expected to be a perfect answer to this problem and matrix materials with progressively complex response need to be examined to develop a good understanding of lateral gauge response. What is clear is that if the direct problem is solved successfully, that is--if a matrix constitutive model is constructed that can then be used to give good agreement between the calculated and the measured gauge response, then reasonable confidence can be placed in the model describing the matrix material.

III. PUBLICATIONS, PRESENTATIONS, AND ASSOCIATED PERSONNEL

A. Publications

The following papers have been published to date.

1. D. Y. Chen, Y. M. Gupta, and M. H. Miles, "Quasi-static Experiments to Determine Material Constants for Piezoresistance Foils Used in Shock Wave Experiments," J. Applied Phys. 55, 3984-3993 (1984).*
2. S. C. Gupta and Y. M. Gupta, "Piezoresistance Response of Longitudinally and Laterally Oriented Ytterbium Foils Subjected to Impact and Quasi-static Loading," J. Applied Phys. 57, 2464-2473 (1985).
3. N. S. Brar and Y. M. Gupta, "Piezoresistance Response of Different Batches of Ytterbium Foils," in *Shock Waves in Condensed Matter*, page 513, Editor Y. M. Gupta (Plenum Publishing, New York, 1986).

The following manuscripts have been submitted to the Journal of Applied Physics for publication and are attached here as appendices.

1. Y. M. Gupta and S. C. Gupta, "Incorporation of Strain Hardening in Piezoresistance Analysis: Application to Ytterbium Foils in a PMMA Matrix."*
2. N. S. Brar and Y. M. Gupta, "Piezoresistance Response of Ytterbium Foil Gauges Shocked to 45 Kbar in Fused Silica Matrix."

The following manuscript is currently under preparation for submission to the Journal of Applied Physics.

S. C. Gupta and Y. M. Gupta, "Effect of Matrix Properties on the Piezoresistance Response of Ytterbium Foils,"

---

* These publications were supported partially by the AFOSR Grant.

B. Presentations

The following invited talks, based in part on the AFOSR work, were presented by the principal investigator:

1. "Can Piezoresistance Gauges be Used to Obtain Time-Resolved Stress Measurements in Shock Wave Experiments," Third American Physical Society Topical Conference on Shock Waves in Condensed Matter, Santa Fe, NM (July, 1983).
2. "Recent Developments in Understanding Piezoresistance Gauge Measurements," Presentations given at DNA Headquarters (Hosted by Dr. M. Frankel and attended by personnel from DNA, Kirtland AFB, BRL, and SRI International) and at NSWC, Silver Spring, MD (Hosted by Dr. J. W. Forbes and attended by personnel from the Detonation Physics branch). Both of these talks were given in the first week of April, 1984.
3. "Use of Piezoresistance Gauges to Measure Material Properties under Shock Loading," Presented at the Nitro-Nobel Basic Research Institute, Bangalose, India (January, 1985). This is a small research organization that is involved primarily with the development of high explosives for commercial application.
4. "Recent Developments in Dynamic Stress Measurements," Presented at the Air Force Weapons Laboratory, Albuquerque, NM (September, 1985). Hosted by Dr. T. Ross and attended by personnel from AFWL, University of New Mexico, and AFOSR.
5. "Stress Measurements for Improved Constitutive Models." Seminar at the University of California, San Diego, Department of Applied Mechanics and Engineering Science (January, 1986). Hosted by Dr. S. Nemat-Nasser and attended by faculty and graduate students of the department.

The following contributed talks, supported in part by AFOSR, were presented at scientific meetings as indicated:

1. S. C. Gupta and Y. M. Gupta, "Response of Ytterbium Foils Oriented Parallel and Perpendicular to the Shock Front," Third APS Topical Conference on Shock Waves in Condensed Matter, Santa Fe, NM (July, 1983).
2. D. Y. Chen, M. H. Miles, and Y. M. Gupta, "Determination of Piezoresistance and Mechanical Constants for Piezoresistance Foils Used in Shock Wave Experiments," Third APS Topical Conference on Shock Waves in Condensed Matter, Santa Fe, NM (July, 1983).

3. S. C. Gupta and Y. M. Gupta, "Effect of Matrix Properties on the Piezoresistance Response of Ytterbium and Manganin," Spring Meeting of the American Physical Society, Washington, D.C. (April, 1984).

4. N. S. Brar and Y. M. Gupta, "Resistance Change of Ytterbium Foils Subjected to Quasi-static and Dynamic Stresses," Fourth APS Topical Conference on Shock Waves in Condensed Matter, Spokane, WA (July, 1985).

In addition, the principal investigator has had extensive discussions with personnel from various organizations (SRI International, Lawrence Livermore National Laboratory, Naval Surface Weapons Center, AFWL) to transfer knowledge gained from the work performed under the AFOSR grant to their applications of interest.

C. Professional Personnel

The following Postdoctoral Research Associates have been supported in part during the course of this grant.

1. Dr. S. C. Gupta (Ph.D. in Physics from the University of Bombay, India)
2. Dr. D. Y. Chen (Ph.D. in Materials Science from the University of Virginia, USA)
3. Dr. N. S. Brar (Ph.D. in Geophysics from the University of Western Ontario, Canada)

In addition to these individuals, significant contributions were made to the experimental effort by Mr. Martin Williams (Engineering Associate) and Mr. Jerry Thompson (Engineering Technician).

IV. CONCLUDING REMARKS

The work completed and summarized in this report has resulted in an in-depth understanding of piezoresistance gauge response under shock loading. The phenomenological model developed to analyze and interpret piezoresistance measurements has been successful beyond our original expectations. Well characterized laboratory experiments were designed and performed to evaluate various aspects of the phenomenological model; good agreement between calculations and experiments was observed.

The development of a quasi-static method and related analysis to obtain the complete set of electromechanical constants necessary to characterize the foils is expected to be of considerable practical significance in using piezoresistance gauges to measure high strain-rate material response. The quasi-static methods will not eliminate shock wave calibration experiments but should result in a significant reduction of these experiments.

All of the effort to date has been spent on the direct problem, that is--understanding the gauge response in well characterized matrix materials. This is a necessary step before studying more complex materials. The good success in the present work suggests that future efforts, using the developments summarized here, should be directed at studying more complex materials by attempting to model the gauge response in materials that display rate-dependent, multiple wave structure under shock loading. Using a self-consistent approach it would be very desirable to infer the material constitutive behavior from gauge measurements.

Finally, an important need exists to transition the results of this basic research effort to field applications including non-planar loading conditions. At present, piezoresistance gauges provide the most reliable means for stress measurements at high stresses under dynamic loading. Given the time and costs involved in such experiments, it is important that gauge packages be optimally designed and the measurements be properly analyzed. This transition task is non-trivial and will require considerable coordination and interest on the part of various groups.

REFERENCES

1. R. A. Graham and J. R. Asay, High Temp. - Pressures 10, 355 (1978).
2. Y. M. Gupta, "Analysis and Modeling of Piezoresistance Response", DNA Report 5451F (1980).
3. Y. M. Gupta, J. Appl. Phys. 54, 6094 (1983).
4. Y. M. Gupta, J. Appl. Phys. 54, 6266 (1983).
5. J. D. Eshelby, Proc. Royal Soc. London A241, 376 (1957).
6. S. C. Gupta and Y. M. Gupta, J. Appl. Phys. 57, 2464 (1985).
7. Y. M. Gupta, D. D. Keough, D. Henley, and D. F. Walter, Appl. Phys. Lett. 37, 395 (1980).
8. D. Y. Chen, Y. M. Gupta, and M. H. Miles, J. Appl. Phys. 55, 3984 (1984).
9. Y. M. Gupta and L. Seaman, "Local Response of Reinforced Concrete to Missile Impact", EPRI Report NP-1217 (1979).
10. D. D. Keough and J. Y. Wong, J. Appl. Phys. 41, 3508 (1970).
11. N. S. Brar and Y. M. Gupta, "Piezoresistance Response of Different Batches of Ytterbium Foils", in *Shock Waves in Condensed Matter*. Editor Y. M. Gupta (Plenum Publishing, New York, 1986).

APPENDIX 1

INCORPORATION OF STRAIN-HARDENING IN PIEZORESISTANCE ANALYSIS: APPLICATION TO YTTERBIUM FOILS IN A PMMA MATRIX

Y.M. Gupta and Satish C. Gupta*

Shock Dynamics Laboratory

Department of Physics

Washington State University

Pullman, WA 99164-2814

ABSTRACT

The results of an earlier paper are extended to include strain-hardening in the analytic model for piezoresistance. This development is necessary to model the gauge hysteresis observed in the experimental data. Analytic developments to incorporate strain-hardening in the theoretical formalism and procedures to calculate the gauge response are described. The analytic model is used to calculate the response of ytterbium foils in PMMA matrix in both shock wave and quasi-static experiments. Good agreement is observed between the model predictions and experimental results. Difficulties in calculating the lateral gauge response when the matrix material is inelastic are discussed.

* Current Address: Neutron Physics Division, BARC, Bombay 400 085, INDIA.

I. INTRODUCTION

In earlier studies a theoretical framework to analyze and interpret piezoresistance gauge measurements was developed.[1,2] The analytic developments consisted of a phenomenological electromechanical model for piezoresistance and an elastic-plastic inclusion analysis. The general features of piezoresistance gauge response under shock loading could be explained, in principle, using this approach. Detailed comparisons between theory and experiment were precluded because a very limited amount of relevant data were available.[3] In the earlier work, the gauge was assumed to be an elastic-perfectly plastic inclusion. The limitations of this assumption were recognized but it was adopted because of resulting simplifications in the analysis, and a lack of needed material property data on the gauge foils.

Since this theoretical effort, extensive shock wave data have been obtained on ytterbium and manganin foils in various matrix materials.[4-8] In addition, methods have been developed to measure materials constants for gauge foils of interest.[9] These results have demonstrated that the elastic-perfectly plastic assumption is inadequate; the piezoresistance gauge needs to be modeled as an elastic-plastic-strain hardening inclusion to correctly model the observed gauge hysteresis. Although gauge hysteresis is a problem of long standing in the use of piezoresistance gauges in shock wave studies, it has been treated primarily in an empirical manner.[10] A systematic analysis and modeling of residual resistance (or hysteresis) is necessary for accurate interpretation of piezoresistance measurements particularly during unloading and reloading.

In this paper we have extended the earlier work[2] to include strain-hardening and then used the analytic model to analyze piezoresistance data from ytterbium foils encapsulated in PMMA matrix.[5] Application to other combinations of matrix materials and foils will be reported in subsequent publications. In Section II, the earlier theoretical work is summarized briefly and the theoretical relations to incorporate strain-hardening are derived. In Section III, data from both dynamic and quasi-static

experiments are analyzed and discussed. The conclusions of the present work are presented in Section IV. Details pertinent to the theoretical formalism are presented in the Appendices.

II. THEORETICAL DEVELOPMENTS

A. Summary of the Existing Model[1,2]

The phenomenological model for calculating the resistance change of a gauge element subjected to an inelastic deformation is used to obtain the expression:

$$\frac{\Delta R_3}{R_{30}} = \left[\pi_{11}\Delta\sigma_3 + \pi_{12}\left(\Delta\sigma_1 + \Delta\sigma_2\right) + \eta\Delta\gamma^p\right] + \Delta\epsilon_3 - \Delta\epsilon_2 - \Delta\epsilon_1 \qquad (1)$$

Where x_1 axis is along the gauge width, x_2 axis is along the gauge thickness, and x_3 axis is along the gauge length. σ and ϵ represent the stress and strain tensor, respectively, in the gauge foil. γ^p is a scalar measure of strain hardening that is taken to be $\sqrt{I'^p_2}$ $\left(= \sqrt{1/2\epsilon'^p_{ij} \cdot \epsilon'^p_{ij}}\right)$. π_{11} and π_{12} are piezoresistive coefficients similar in form to elastic constants. The terms involving stress can also be expressed in terms of constants, $\alpha = \pi_{12}$ and $\beta = (\pi_{11} - \pi_{12}) / 2$ that are similar to Lame's constants. The constant η relates the amount of plastic deformation, $\Delta\gamma^p$, to permanent changes in the gauge resistivity and has been termed as the "electrical strain hardening" coefficient. The results presented in the earlier work[2] were based on the assumption of $\eta = 0$. The assumptions used in deriving the above incremental expression have been discussed in Reference 2 and are not repeated here.

The stresses and strains appearing in Eq. (1) are not independent, but are coupled through the mechanical constitutive relation for the material. The main elements of this model are described in the next sub-section. The paper by Chen, et al.[9] describes a quasi-static method and related analyses to evaluate the complete set of linear piezoresistive and mechanical constants that appear in the theoretical formalism. Results for ytterbium, manganin, and constantan foils are presented in Reference 9.

The second part of the earlier analytic work consisted of relating the gauge stresses and strains to the

matrix mechanical state. This part termed the "inclusion problem" consisted of extending the Eshelby solution for an ellipsoidal elastic inclusion in an elastic matrix[11] to an elastic-plastic inclusion. The essential elements of this analysis using the summation convention can be expressed in the matrix notation as:[2]

$$\left[(H''_{im} - H_{im}) \cdot S_{mp} + H_{ip}\right] \cdot \epsilon_p{}^T = \left[H_{in} - H'_{in}\right] \cdot \epsilon_n{}^A \tag{2}$$

$$\epsilon_l{}^C = S_{lm}\epsilon_m{}^T \tag{3}$$

$$\epsilon_m = \epsilon_m{}^C + \epsilon_m{}^A \tag{4}$$

$$\sigma_p = H''_{pq} \cdot \epsilon_q \tag{5}$$

Where σ = stress in the inclusion , ϵ = strain in the inclusion, ϵ^A = applied matrix strain, ϵ^T = stress free transformation strain, ϵ^C = constrained strain, S = tensor that depends on the Poisson's ratio of the matrix and the shape of the inclusion, H = modulus tensor of the elastic matrix, and H'' = modulus tensor of the inelastic inclusion. In the past work, determination of H'' in the plastic regime was simplified because the perfectly plastic state could be modeled by setting the shear modulus, $G = 0$, in the plastic state. An incremental approach was developed, assuming S to be constant, to obtain the gauge stresses and strains during loading and unloading.

The applied matrix strain, ϵ^A, is specified and the above equations are solved, in the order presented, to get σ and ϵ in the inclusion. Below the yield limit of the inclusion, the modulus tensor, H'', reduces to the elastic modulus tensor for the inclusion, H'. Equations (2) - (5) though simple in form are quite cumbersome to solve for a particular problem.

B. Incorporation of Strain-Hardening in the Gauge Response

To evaluate the resistance change in Eq. (1) for the more realistic case considered here, we first need to determine the stresses, strains, and the plastic strain at different stages of the foil deformation. These coupled with a knowledge of the material constants π_{11}, π_{12}, and η can then be used to calculate the foil response for an applied matrix strain. In the remainder of this section, we describe the procedure for determining the modulus tensor, H'', for a strain-hardening inclusion, and the calculation procedure for evaluating σ, ϵ, γ^p. The determination of the material constants for a specific application is discussed in the next section.

1. Constitutive Model

The constitutive model used to construct the modulus tensor, H'', for a strain-hardening foil is based on the usual postulates of rate-independent plasticity theory[12,13] : (a) existence of a yield surface and (b) the flow rule for determining plastic strains. In addition, we assume an isotropic response and a pressure-independent yield surface because our interest is in polycrystalline metallic foils. The incremental equations governing the elastic-plastic-hardening response, using the summation convention, are:

Additivity of elastic and plastic strain increments

$$d\epsilon_{ij} = d\epsilon^e{}_{ij} + d\epsilon^p{}_{ij} \tag{6}$$

Incremental Hooke's law for elastic strains

$$d\sigma_{ij} = \left(K - \frac{2G}{3}\right) d\epsilon^e{}_{mm}\delta_{ij} + 2G d\epsilon^e{}_{ij} \tag{7}$$

von-Mises yield surface with strain hardening

$$f = \sqrt{J'_2} - Y_o - M\gamma^p = 0 \tag{8}$$

Flow rule for determining plastic strains

$$d\epsilon^p{}_{ij} = d\lambda \frac{\partial f}{\partial \sigma_{ij}} \tag{9}$$

Where K = bulk modulus, G = shear modulus, $J'_2 = \frac{1}{2}\sigma'_{ij} \cdot \sigma'_{ij}$ and σ'_{ij} is the stress deviator[13], Y_o = experimentally determined yield stress expressed in terms of $\sqrt{J'_2}$, M is the measured strain hardening coefficient,[9] and $d\lambda$ is a non-negative scaler that is determined by the amount of strain hardening. Although the constitutive model used here is relatively simple it appears to be satisfactory for our analysis as discussed in Section III.

In our work, we assume that Y_o also marks the onset of permanent changes in the electrical resistivity. This assumption is supported by the experimental results described in Reference 9.

2. Determination of the Modulus Tensor H''

The objective is to find an incremental relation between the foil stresses and strains in the plastic range. The results presented here are based on the plasticity analysis used in earlier studies.[14,15] The derivations, though tedious, involve straightforward tensor manipulation using multi-dimensional plasticity relations.

It is convenient to separate Eq. (7) in terms of mean stress and stress deviators using Eq. (6), and the condition of plastic incompressibility ($d\epsilon^p{}_{mm} = 0$) that follows from Eqs. (8) and (9). Recall, $\sigma'_{ij} = \sigma_{ij} - \frac{\sigma_{mm}}{3}\delta_{ij}$.

$$d\sigma_{mm} = 3K\ d\epsilon_{mm}{}^e = 3Kd\epsilon_{mm} \tag{10}$$

$$d\sigma'_{ij} = 2G\ (d\epsilon'_{ij} - d\epsilon^p{}_{ij}) \tag{11}$$

By differentiating the expression for f in Eq. (8), we can write[16]

$$\frac{\partial f}{\partial \sigma_{ij}} = \frac{\sigma'_{ij}}{2\sqrt{J'_2}} \tag{12}$$

Using Equations (9) and (12), Eq. (11) can be rewritten as

$$d\sigma'_{ij} = 2G\left[d\epsilon'_{ij} - d\lambda \cdot \frac{\sigma'_{ij}}{2\sqrt{J'_2}}\right] \tag{13}$$

Using the equation for $d\lambda$, derived in Appendix A, we obtain

$$d\sigma'_{ij} = 2G\left[d\epsilon'_{ij} - \frac{G\sigma'_{mn}d\epsilon'_{mn}}{(2G + M)J'_2}\sigma'_{ij}\right] \tag{14}$$

Combining this expression with Eq. (10) and recalling that $d\epsilon_{ll}^{p} = 0$, we get the desired relation

$$d\sigma_{ij} = \left(K - \frac{2G}{3}\right)d\epsilon_{ll}\delta_{ij} + 2Gd\epsilon_{ij} - \frac{2G^2\sigma'_{mn} \cdot \sigma'_{ij}}{(2G + M)J'_2}d\epsilon'_{mn} \tag{15}$$

The first two terms in this equation correspond to an elastic response (as if the incremental strain was purely elastic); the third term describes the contribution of strain-hardening to the stress increase. In the absence of strain-hardening ($M = 0$), it is not necessary that each increment, $d\sigma'_{ij}$, be zero. Instead, the isotropic strain-hardening model [Eq. (8)] assumed here requires that $d\sqrt{J'_2} = 0$ if $M = 0$. This is indeed the case and Eq. (15) is correct.

Because of the summation in the third term, it is preferable to evaluate Eq. (15) term by term. Expressing Eq. (15) in the matrix notation as

$$d\sigma_\alpha = H''_{\alpha\beta}d\epsilon_\beta \text{ where } \alpha, \beta, = 1 \text{ to } 6 \tag{16}$$

We have evaluated the components of the modulus tensor, H'', in Appendix B.

3. Determination of γ^p

The resistance change expression in Eq. (1) requires that the accumulated plastic strain γ^p be known during the deformation. In Appendix C, we have shown that

$$d\gamma^p = \frac{d\lambda}{2} \tag{17}$$

Using the expression for $d\lambda$ given by Eq. (A.6) in Appendix A, we can write

$$d\gamma^p = \frac{2G\sigma'_{ij} \cdot d\epsilon'_{ij}}{(2G + M)\sqrt{J'_2}} \tag{18}$$

Hence, for each increment of strain, $d\epsilon_{ij}$, we can calculate $d\gamma^p$. Adding this to the previous value of γ^p, we can keep track of the accumulated plastic strain in the calculation.

C. Calculational Procedure

The resistance change calculation for the foil is performed in two parts: calculation of the mechanical variables and using these to evaluate Eq. (1). The first part of the calculation is briefly discussed here and the second part, including the evaluation of material constants, is discussed in the next section.

The calculations of stresses, strains, and a scalar measure of the accumulated plastic strain in the foil for a given matrix strain are performed using a computer program INCL4. This program is an extension of the program used in the earlier work; the calculational procedure follows closely the procedure described in Section VC. of Reference 2. As before, we assume a plane strain problem and an elliptical cross-section for the foil. These assumptions have been discussed and justified in Reference 2.

In calculating the gauge response for a given matrix strain, the matrix strain is divided into a large number of increments (e.g of the order of 100). Equations (2) - (5) can be expressed in an incremental form if the shape tensor S is taken to be constant. For the strain magnitudes discussed here, this is a good assumption. For a given matrix strain increment, $d\epsilon^A$, Equation (2) is solved to obtain $d\epsilon^T$. Equation (2) represents a set of three simultaneous equations. The S, H, and H' (or H'' for plastic deformation) tensors are calculated from the material properties of the foil and the matrix at that strain. Knowledge of $d\epsilon^T$ permits calculation of $d\epsilon^C$, $d\epsilon$, and $d\sigma$ using Equations (3) - (5). The increments in stresses and strains are added to the previously stored values. If the inclusion stresses are such that the yield limit of the foil material is not exceeded in a particular increment, then the elastic calculation continues for the next strain increment.

If the inclusion stresses at the end of a current cycle exceed the yield limit of the foil then the current cycle is repeated using sub-increments to determine the threshold matrix strain that results in yielding. Beyond the threshold strain, the modulus tensor corresponding to the elastic-plastic-strain hardening response, H'', is used to calculate the stresses and strains in the foil, and Equation (18) is used to calculate the plastic strain increment. Because of possible changes in the direction of loading in the matrix (unloading and reloading), care needs to be taken in determining the onset of yielding in the foil. We have chosen the plastic strain measure to be a monotonically increasing function, irrespective of the loading direction in the matrix.

In the Eshelby method, the matrix is required to have a linear stress-strain relation. In the present work, this requirement is met by choosing a longitudinal modulus that gives the correct peak longitudinal stress for a prescribed uniaxial strain in the matrix. Hence, the peak state is given by a point on the Hugoniot of the material. The choice of a linear longitudinal modulus for a particular peak stress is equivalent to loading along the Rayleigh line. Because the Raleigh line is the actual loading path of a shocked material element, our procedure is satisfactory for the present purposes. Further separation of the longitudinal modulus into bulk and shear moduli is discussed in Section IV.B.

During unloading the matrix is assumed to unload along the Hugoniot and an appropriate longitudinal modulus, valid for unloading from a particular peak strain, is chosen to determine the residual stresses and strains in the gauge foil. If the foil does not undergo inelastic deformation, these quantities will be zero.

The above procedure for calculating the loading and unloading moduli, though reasonable, cannot be justified rigorously. We believe that this procedure is satisfactory because the inclusion quantities depend primarily on the end states and are relatively insensitive to small variations in the loading/unloading path. This was verified by performing several parameter variation calculations.

III. ANALYSIS OF EXPERIMENTAL RESULTS AND DISCUSSION

The theoretical formation developed in the last section is used to analyze the experimental results from dynamic and quasi-static uniaxial strain experiments reported in Reference 5.

A. Summary of Experiments[5]

In both the dynamic and quasi-static experiments, π-shaped ytterbium foil gauges were embedded in a PMMA matrix into grooves of nearly matching dimensions (see Figures 1 and 3 in Reference 5). The embedded gauges had two orientations -- parallel and perpendicular to the direction of uniaxial strain in the PMMA matrix. Resistance change measurements for the two gauge orientations were obtained as a function of matrix longitudinal stress in both dynamic and quasi-static experiments. The maximum longitudinal matrix stress was 25 kbar for the dynamic experiments and 4 kbar for the quasi-static experiments.

Because the emphasis of our work is on dynamic experiments, a typical record from a longitudinal gauge in one of our gas-gun experiments is shown in Figure 1. This resistance change-time profile is for a peak longitudinal matrix stress of 11.6 kbar and is close to the longitudinal wave profile expected from the shock wave uniaxial strain response of PMMA.[17] The profiles from lateral gauges are similar but display larger rise times and some oscillatory response superposed on the flat top peak (see Figure 4 in Reference 5). Both sets of gauges show non-zero residual resistance change even when the longitudinal matrix stress is unloaded to a zero value. This observed residual resistance change or gauge hysteresis is plotted as a function of the peak longitudinal matrix stress in Figure 2. The broken vertical lines are drawn to indicate three regions: in region I there is no gauge hysteresis; in region II the residual resistance curve shows a near-parabolic increase; at approximately 7.6 kbar, the onset of region III, the residual resistance increases very rapidly and then reaches a constant value. These results are analyzed and discussed later in this section.

B. Determination of Material Parameters for the Analytic Model

1. Mechanical Properties of PMMA and Yb.

The mechanical properties of PMMA under shock loading were taken from the papers by Barker and Hollenbach[17], and Gupta.[18]. As indicated at the end of Section II, the loading path for PMMA is taken to be along the Rayleigh line corresponding to the Hugoniot given by Barker and Hollenbach.[17] The longitudinal modulus, determined by the slope of the Rayleigh line, is divided into bulk and shear moduli using the shear modulus values given by Gupta.[18] The unloading path for the PMMA is taken to be along the Hugoniot and the following expression was used in our calculations

$$K_L = 97 + 400\epsilon \text{ , } kbar \tag{19}$$

where ϵ is the peak strain for a given experiment. The linear unloading path given by Eq. (19) averages the actual nonlinear unloading path for a particular shock experiment. A series of parameter sensitivity calculations showed that the residual resistance of the gauge was relatively insensitive to the unloading modulus. However, care needs to be exercised in modeling the unloading response from stress levels that are beyond the threshold for inelastic deformation in PMMA. This point will be clarified later in our analysis of the residual resistance data shown in Figure 2.

Because of the viscoelastic response of PMMA, the moduli for quasi-static experiments are significantly different from the high strain-rate moduli. The results of Stephens, et. al.[19] are used to determine the moduli pertinent to the quasi-static experiments.

The material constants used to describe the elastic-plastic-strain hardening response of Yb. foils were measured in the work of Chen, et. al.[9] and are presented in Table I. The yield stress value cited in Table I can be written in terms of $\sqrt{J'_2}$ $\left(= \sigma_1 / \sqrt{3} \right)$ as 0.47 kbar. However, to get the correct stress threshold for residual resistance in the dynamic experiments (see Figure 2), we had to use the $\sqrt{J'_2}$ value corresponding to the onset of inelastic deformation and not the 0.2% offset value cited in

Table I. Hence, our calculations use a yield value of $\sqrt{J'_2}$ = 0.28 kbar for ytterbium. The linear strain-hardening coefficients given in Table I is obtained from experimental data that extend to 2-3 percent strain.[9] Thus, care needs to exercised in using the cited hardening coefficient value at strains beyond this range. For use at higher strains, it would be preferable to fit the data in Reference 9 using a parabolic hardening curve.

2. Electromechanical Constants for Yb. foils.

The electromechanical constants (π_{11}, π_{12}, and η) cited in Table I need to be reexamined for use in shock wave experiments for the following reasons: stress dependence of π_{ij} because of the strongly nonlinear response of ytterbium, and the validity of the η value determined from quasi-static work for shock wave experiments. The determination of η from shock data is considered first.

In the development of the piezoresistance model[1,2], η was defined as the material parameter that related resistivity changes to plastic deformation (at a constant stress). Hence, it is a phenomenological parameter that determines irreversible changes in resistivity due to the production of lattice defects. From shock wave data on metallic foils[20] and metals[21], it has been established that shock deformation results in enhanced defect production. Hence, we expect η in shock experiments to be higher than that cited in Table I. We have developed a procedure for evaluating η by rewriting Eq. (1), in the limit of small stress and strains, as

$$\eta = \frac{1}{\gamma^p}\left[\frac{\Delta R_3}{R_o} - \pi_{11}\sigma_3 - \pi_{12}(\sigma_1 + \sigma_2) - \epsilon_3 + \epsilon_1 + \epsilon_2\right] \tag{20}$$

This equation is used to evaluate η from the residual resistance data for the longitudinal gauge as follows. The inclusion calculation is performed to obtain the stresses, strains, and the accumulated plastic strain upon unloading from the peak matrix stress corresponding to a particular experiment. Because the residual stresses and strains in the gauge are very small, we can use the small stresses and strain approximation, and the linear piezoresistive coefficients on the right side of Eq. (20). The

resistance change value in Eq. (20) is the residual value obtained from the experiments. We can then determine η as a function of plastic strain. Results of this calculation are shown in Table II and a plot of η vs. γ^p is shown in Figure 3.

Because η is a material property, the values in Table II correspond to the particular batch of foils used in our work. The determination of η using Eq. (20) in the present work, assumes that the matrix away from the inclusion is stress free upon unloading. If this is not the case then the stress and strains in Eq. (20) are not entirely due to the gauge plasticity and our procedure is not valid. This appears to be the case for the experimental result at 7.4 kbar in Table II, that is -- matrix inelastic effects appear at this stress. For this reason we have chosen not to calculate η from the higher stress experiments. It is difficult to make error estimates for η because of the complicated nature of the calculation and the different material assumptions. The asymptotic value of η in Figure 3 is close to the quasi-static value of 1.13 obtained in Reference 9.

Residual resistance data even for an inelastic matrix can be analyzed using Eq. (20) because it is a general equation. However, the proper inclusion analysis is required to handle the nonlinear response of the matrix and to include the correct constitutive description for the inelastic matrix. These requirements will necessitate the use of a numerical procedure using finite element techniques.[22]

The piezoresistive response of ytterbium is strongly nonlinear and requires that either π_{ij} be made stress dependent or we use higher order constants. The derivation[2] of π_{ij} involved a Taylor's series expansion, and incorporation of the next order terms would lead to three extra constants in the theoretical formalism for an isotropic material. (This development is very similar in form to the elastic constant formulation.) Although such a development is straightforward, it is expected to be of minimal value because of the difficulty in evaluating the higher order constants with reasonable accuracy. To keep the formalism simple, we chose to consider the following expressions for π_{ij}

$$\pi_{11} = \pi^{o}_{11} + AP \tag{21}$$

$$\pi_{12} = \pi^{o}_{12} + BP \tag{22}$$

where the linear values in Table I correspond to zero pressure ($P = -\sigma_{mm}/3$), and A and B give the pressure dependence. In principle, Equations (21) and (22) can be combined with Eq. (1) to give an expression that can be used to evaluate A and B from different experiments. To get all the stresses and strains in the resulting equation requires the use of the inclusion analysis. Despite several attempts at calculating A and B, we were unsuccessful because of the very small differences in the inclusion stresses. The low value of yield stress for the ytterbium results in a nearly singular set of equations. Because of the nearly isotropic state of stress in the foils, we chose $A = B$ and derived the following pressure coefficient by averaging results from several experiments.

$$A = B = 7.6 \times 10^{-3} \ kbar^{-2} \tag{23}$$

C. Comparison of Calculated Results and Experimental Data

1. Dynamic Experiments

The residual resistance data from longitudinal gauges, shown in Figure 2 match the calculations very well to 7.4 kbar, as expected. This is because the η values were derived from these data. Hence, the calculated curves are not shown. Beyond the elastic limit of the matrix, our calculations are not valid. Although a comparison of calculated results, assuming an elastic matrix, with the data shown in Region III in Figure 2 is helpful in estimating residual matrix stresses due to matrix inelasticity, to data we have not developed a satisfactory procedure for inverting the data in Figure 2 to calculate the residual matrix stresses.

The residual resistance curve for the lateral gauge in Figure 2 can only be discussed qualitatively, and detailed comparisons with model calculations are not feasible because of the following reasons.

As indicated in the earlier paper,[2] the inclusion calculations show that during unloading tensile stresses develop between the matrix and the inclusion. These stresses can lead to a separation between the gauge and the matrix, and violate the basic assumption of the welded interface between the matrix and the gauge in our calculations. The extent of the separation is difficult to determine either analytically or experimentally. The non-negative residual values from the lateral gauge in Figure 2 in the elastic regions of the matrix suggest that tensile stresses are being relaxed. Also, the lateral gauge data are below the longitudinal data as expected (see Figure 4 in Reference 2). Above the elastic limit of PMMA, the lateral stresses in the PMMA are non-zero and compressive. Hence, the lateral gauge values are expected to be higher in comparison to the longitudinal gauge values. This is indeed observed in Figure 2.

The peak resistance change for both gauge orientations were calculated using the analytic model, and the results are shown in Figure 4. Experimental results from Reference 5 are shown to provide a comparison between the model calculations and the experiments. Calculated curves up to the elastic limit of the PMMA are shown as solid lines. Good agreement is seen between the model calculations and the data including the cross-over between the lateral and longitudinal gauge data. The good agreement observed in Figure 4 demonstrates the validity of our overall approach. Because most of the material parameters were based on quasi-static measurements, the analytic model provides a link between quasi-static and dynamic experiments. In performing these calculations, the η values corresponding to γ^p at the peak stress were determined from Figure 3..

Above the 7.6 kbar threshold for PMMA, our analytic model is not rigorously valid. This is because PMMA cannot be modeled as a linear material (for a particular experiment) and the constitutive response of PMMA is not accurately known under dynamic loading. Despite these limitations, we have calculated the longitudinal gauge response at higher peak stresses for the following reasons: (i) The longitudinal stress-strain curve in PMMA is well established[17]. (ii) Because of the continuity of longitudinal stress[2] in PMMA and ytterbium, the longitudinal stress in ytterbium is also known

accurately. (iii) The small value of yield stress in ytterbium leads to a stress state in the foil that is governed primarily by the longitudinal stress in the matrix; the lateral stresses in the matrix have negligible effects, and (iv) Because of the large values of π_{ij}, the response of ytterbium at stresses above a few kilobar is governed primarily by the stress terms in Eq. (1).

The calculations, shown as a broken line in Figure 2, show a fairly good agreement with the experimental results up to a matrix stress of 18-19 kbar. Beyond this value, the ytterbium appears to undergo a change in its physical properties[5,23] and the piezoresistance model used here is no longer valid for ytterbium. Below 19 kbar, the difference between the calculations and experiments is only slightly larger than the experimental scatter; the experimental values being higher. The higher values in the experiments are expected because we are not able to account for the resistance change in the gauge foils due to inelastic deformation in the matrix. This is the same reason that we calculate a smaller residual resistance change in the foils beyond 7.5 kbar in comparison to the experimental data. By estimating the difference using the elastic matrix calculation based on Figure 3 and the actual residual values observed in Figure 2, we have determined that this difference is approximately $\frac{\Delta R}{R_o} = 0.05 \pm 0.02$. Incorporating this difference in Figure 4 brings the agreement between the calculations and experiments to well within experimental scatter.

Because of the reasons listed earlier, we have been quite successful in using the analytic model to simulate the longitudinal gauge data beyond 7.6 kbar. However, many of these reasons are not applicable for lateral gauges and we cannot calculate the lateral gauge response beyond the elastic limit of PMMA. Based on the calculations in the elastic range of PMMA, it appears that the lateral gauge response is related mainly to the lateral stresses in PMMA. However, without independent experimental corroboration or additional analysis, it is not possible to calculate the lateral gauge response in the inelastic range. Preliminary two-dimensional dynamic and quasi-static calculations by Ito, et. al.[22] suggest that unlike the longitudinal gauge, the lateral gauge response is dependent on the gauge-

matrix boundary conditions and may require a wave propagation or transient analysis under certain loading conditions. We believe that modeling the lateral gauge response in an inelastic matrix will require an iterative procedure as discussed in Section IV.C. in Reference 5.

2. Quasi-static Experiments

The experimental results from our earlier quasi-static uniaxial strain experiments[5] are shown in Figure 5. The noteworthy feature is that the lateral gauge data are higher than the longitudinal gauge data. Although they appear to be approaching an intersection (a smooth extrapolation results in an intersection around 5 - 5.5 kbar), no intersection is observed up to 4 kbar. This is in contrast to the dynamic data that show an intersection around 2 kbar (Figure 2). To model these results, we used the material properties of PMMA from the quasi-static, triaxial data of Stephens, et. al.[19] Except for the presence of piezoresistance gauges, our experiments were comparable to the work cited in Reference 19. The electromechanical properties of the ytterbium foils were not available because these data were from a batch of foils[24] that were used up prior to the developments reported in Reference 9. Hence, we used the foil properties listed in Table I. The η and yield stress values were varied to give good agreement with the longitudinal gauge data. The same set of constants (η = 0 and yield stress = 0.38 kbar) were then used to calculate the lateral gauge response. The calculated response for the two orientations is shown as solid lines in Figure 5 and excellent agreement can be observed.

The agreement in Figure 5 for either orientation can be questioned because the absolute values of the foil constants were not known to us. The significant aspect of the results shown in Figure 5 is the ability to model the relative differences for the two gauge orientation using a single set of constants. The lack of a cross-over in the gauge data for the two orientations is readily explained using the model calculations. The cross-over occurs because of plastic yielding in the gauge.[2] Under quasi-static loading, the PMMA displays a more compliant response (larger Poisson's ratio) in contrast to the impact experiments. This behavior results in lower stress deviators in the gauge for a given longi-

tudinal matrix stress. Hence, the ytterbium foils yield at a higher matrix stress in comparison to the dynamic experiments. On the basis of the analytic model, we make several related observations: the foils yield prior to the cross-over point; the threshold matrix stress for yielding in the ytterbium is different for the two orientations; the lateral gauge yields at a lower matrix stress because of the higher stress concentration factor in the elastic inclusion problem discussed in Reference 2.

D. Discussion

The results described in the last sub-section have provided a link between quasi-static characterization of piezoresistance foils[9] and their response under shock loading. This is an important development because results from different foil batches (hence, having different material constants) can be systematically compared through the analysis presented here. In a recent paper by Brar and Gupta[6], the shock response of longitudinal ytterbium gauges from a different batch than the batch used in Reference 5 was examined. The matrix material was again PMMA. The experimental results[6] showed higher $\Delta R/R_o$ values in contrast to the data from Reference 5 reproduced here in Figure 4. Using the quasi-static characterization method[9] and the analysis described in the present paper, the gauge response for the second batch of foils was calculated. The calculated curve for the second batch of foils gave higher resistance values than the curve shown in Figure 4; the differences in the two calculated curves were in good agreement with the differences observed in the experimental data.[6] These results provide further support to the analysis and approach described in the present paper.

The use of piezoresistance gauges for complex wave profiles has often been questioned because of the difficulty in incorporating gauge hysteresis into the data analysis. Previous attempts to address this problem have been primarily empirical in nature.[25–27] The procedure described in the present paper provides a systematic method of evaluating and quantifying gauge hysteresis effects for shocked piezoresistance foils. The validity of this approach to other combinations of foil and matrix

materials has also been demonstrated.[7,8] An important aspect of the residual resistance analysis is the ability to quantify the relative contributions to the residual resistance. Examination of Eq. (20) shows that there are three distinct contributors to residual resistance: residual stresses in the gauge, residual strains in the gauge, and accumulated plastic strains. For a purely elastic matrix, these contributions are entirely due to gauge inelasticity. However, for an inelastic matrix (see region III in Figure 2), contributions to these terms can also result from residual stresses and strains in the matrix. Quantitative separation of matrix and gauge effects will require the use of more than one type of gauge foil. This question will be examined in a subsequent study.

The quasi-static results presented in Figure 5 demonstrate the importance of the inclusion analysis and gauge plasticity. Although the matrix longitudinal stress is higher than the matrix lateral stress, the resistance change values for the two orientations show the opposite result. Use of an empirical expression relating the resistance change of the gauge to the stress component normal to the foil, as is commonly done, would give the wrong answer. However, the use of the inclusion analysis predicts the correct answer as shown in Figure 5.

IV. CONCLUDING REMARKS

The developments presented in this paper have resulted in a comprehensive description of piezoresistance response under shock compression. The good quantitative agreement between the model predictions and the experimental results is gratifying and suggests that gauge hysteresis can be incorporated satisfactorily into the analysis. The main results of the present work are as follows:

1. The existing phenomenological model for piezoresistance has been extended to incorporate isotropic strain-hardening in the gauge response.

2. Procedures for analyzing the residual resistance data from gauge foils embedded in an elastic matrix are described. Using this method the material constant, η, describing gauge hysteresis is evaluated. An increase in the gauge residual resistance beyond that caused by gauge inelasticity is due to inelastic deformation of the matrix. However, a specific method to determine the residual stresses and strains due to matrix inelasticity has not been developed to date.

3. Using the theoretical developments presented here and the material constants obtained from foil characterization experiments, good agreement was obtained between model predictions and experimental results for the two gauge orientations in both shock wave and quasi-static experiments. Modeling of the lateral gauge is limited to the stress range where the matrix remains elastic. The results from the quasi-static experiments in the PMMA matrix demonstrate the importance of the inclusion analysis.

The developments presented here have recently been applied to various combinations of gauge materials (ytterbium, manganin) and matrix materials (polycrystalline Al_2O_3, fused silica, PMMA, liquid CS_2). Results from these studies, to be published shortly, show good overall agreement between the model predictions and experimental results. The work to date has resulted in a fairly

rigorous understanding of the longitudinal gauge response and a limited understanding of lateral gauge response. The difficulties in modeling the lateral gauge response in inelastic materials have been described in Reference 5; this problem will be the subject of future studies.

Finally, we mention two aspects of our experimental work that conform closely to the requirements of the analytic model. These are: the use of a simple π-shaped element in contrast to a grid configuration, and the emplacement of gauge foils in a groove instead of on the surface. The thrust of our work was to understand the gauge response and we feel that these requirements were crucial for achieving this understanding. However, if the intent of the experiment is to use the gauge to measure the longitudinal matrix stress profiles due to inelastic deformation in the matrix, then it may be preferable to use a surface gauge. The use of a surface gauge would minimize differences due to matrix inelastic response at different stresses. However, we do recommend the use of a π-shaped element and in-groove lateral gauges based on our overall findings and experience. In addition, we have found it very helpful to characterize different foil batches using the method described by Chen, et. al.[9].

ACKNOWLEDGEMENTS

N.S. Brar is sincerely thanked for pointing out an error in the numerical program. Discussions with D.D. Keough and Y.M. Ito during the course of the work have been useful. The work described here was supported in part by AFOSR Grant 82-0132 and in part by DNA under Contract 001-83-C-0148.

REFERENCES

1. Y.M. Gupta, "Analysis and Modeling of Piezoresistance Response", DNA Report 5451F, SRI International, Menlo Park, CA 94025 (September, 1980), unpublished.

2. Y.M. Gupta, J. Appl. Phys. *54*, 6256 (1983)

3. Y.M. Gupta, D.D. Keough, D. Henley, and D.F. Walter, Appl. Phys. Lett. *37*, 395 (1980).

4. Satish C. Gupta and Y.M. Gupta, Bull. Am. Phys. Soc. *29*, 741 (1984).

5. Satish C. Gupta and Y.M. Gupta, J. Appl. Phys. *57*, 2464 (1985).

6. N.S. Brar and Y.M. Gupta, "Piezoresistance Response of Different Batches of Ytterbium Foils", in *Shock Waves in Condensed Matter*, Ed. Y.M. Gupta (Plenum Publishing, New York, 1986).

7. Satish C. Gupta and Y.M. Gupta, "Piezoresistance Response of Manganin Foils: Experiments and Analysis", in *Shock Waves in Condensed Matter*, Ed. Y.M. Gupta (Plenum Publishing, New York, 1986). A comprehensive account of this work is currently under preparation.

8. N.S. Brar and Y.M. Gupta, "Piezoresistance Response of Ytterbium Foil Gauges Shocked to 45 kbar in Fused Silica Matrix", paper submitted to J. Appl. Phys.

9. D.Y. Chen, Y.M. Gupta, and M.H. Miles, J. Appl. Phys. *55*, 3984 (1984).

10. M.J. Ginsberg, D.E. Grady, P.S. DeCarli, and J.T. Rosenberg, "Effects of Stress on the Electrical Resistance of Ytterbium and Calibration of Ytterbium Stress Transducers", Final Report, Contract DNA001-72-C-0146, SRI International, Menlo Park, CA 94025 (1973), unpublished.

11. J.D. Eshelby, Proc. R. Soc. London A *241*, 376 (1957).

12. Y.M. Gupta, Acta. Met. *25*, 1509 (1977).

13. Y.C. Fung, *Foundations of Solid Mechanics*, Chapter 6, (Prentice-Hall, New Jersey, 1965).

14. Y.M. Gupta and L. Seaman, "Local Response of Reinforced Concrete to Missile Impact", EPRI Report NP-1217, SRI International, Menlo Park, CA 94025 (October, 1979), unpublished.

15. Y.M. Gupta and E. Privitzer, "Compression and Shear Wave Propagation in Salt and Granite", DNA Report 5058F, SRI International, Menlo Park, CA 94025 (August, 1979), unpublished.

16. $$\frac{\partial f}{\partial \sigma_{ij}} = \frac{\partial f}{\partial \sqrt{J'_2}} \frac{\partial \sqrt{J'_2}}{\partial \sigma_{ij}} = \frac{\partial f}{\partial \sqrt{J'_2}} \frac{\sigma'_{ij}}{2\sqrt{J'_2}}$$
The second step has been derived in the Appendix in Reference 12.

17. L.M. Barker and R.E. Hollenbach, J. Appl. Phys. *41*, 4208 (1970).

18. Y.M. Gupta, J. Appl. Phys. *51*, 5352 (1980).

19. D.R. Stephens, H.C. Heard, and R.N. Schock, "High-Pressure Mechanical Properties of Polymethylmethacrylate", UCID-16007, Lawrence Livermore Laboratory, Livermore, CA 94550 (1972), unpublished.

20. J.J. Dick and D.L. Styris, J. Appl. Phys. *46*, 1602 (1975).

21. W.C. Leslie, "Microstructural Effects of High Strain Rate Deformation", in *Metallurgical Effects at High Strain Rates*, Editors R.W. Rohde, B.M. Butcher, J.R. Holland, and C.H. Karnes (Plenum Publishing, New York, 1973).

22. Y.M. Ito, and Y. Muki, Bull. Am. Phys. Soc. *30*, 1312 (1985).

23. N.S. Brar and Y.M. Gupta, "Phase Transition in Shocked Ytterbium Foils Encapsulated in PMMA and Fused Silica", (unpublished).

24. Y.M. Gupta and D.F. Walter, "Piezoresistance Response of Ytterbium Under Static and Dynamic Loading", Technical Report under AFOSR Contract F49630-81-K-002, SRI International, Menlo Park, CA 94025 (April, 1983), unpublished.

25 D.E. Grady and M.J. Ginsberg, J. Appl. Phys. *48*, 2179 (1977).

26. D.J. Steinberg and D.L. Banner, J. Appl. Phys. *50*, 235 (1979).

27. H.C. Vantine, L.M. Erickson, and J.A. Janzen, J. Appl. Phys. *51*, 1957 (1980).

APPENDIX A

Evaluation of $d\lambda$ in Eq. (13).

The yield surface for the foil material is given by Eq. (8) in Section II as

$$f = \sqrt{J'_2} - Y_o - M\gamma^p = 0 \tag{A.1}$$

To calculate $d\lambda$, we recognize that $df = 0$ for continued plastic deformation, i.e. the stress state is along the yield surface.[14] This leads to

$$df = \frac{\partial f}{\partial \sqrt{J'_2}} d\sqrt{J'_2} + \frac{\partial f}{\partial \gamma^p} d\gamma^p = 0 \tag{A.2}$$

Using the relations $\frac{\partial f}{\partial \sqrt{J'_2}} = 1$, $\frac{\partial f}{\partial \gamma^p} = -M$, and the result $d\gamma^p = \frac{d\lambda}{2}$ derived in Appendix C, Eq. (A.2) can be written as

$$d\sqrt{J'_2} - M\frac{d\lambda}{2} = 0 \tag{A.3}$$

Using the definition of $\sqrt{J'_2}$ $\left(= \sqrt{1/2\sigma'_{ij} \cdot \sigma'_{ij}} \right)$, we can write

$$d\sqrt{J'_2} = \frac{\sigma'_{ij} \cdot d\sigma'_{ij}}{2\sqrt{J'_2}} \tag{A.4}$$

Substituting Eq. (13) from Section II. in Eq. (A.4) gives

$$d\sqrt{J'_2} = \frac{G\sigma'_{ij} \cdot d\epsilon'_{ij}}{\sqrt{J'_2}} - Gd\lambda \tag{A.5}$$

Eliminating $d\sqrt{J'_2}$ between Eqs. (A.3) and (A.5), we get the required result

$$d\lambda = \frac{2G\sigma'_{ij} \cdot d\epsilon'_{ij}}{(2G + M)\sqrt{J'_2}} \tag{A.6}$$

APPENDIX B

Evaluation of the H'' matrix terms

Equation (15) can be expressed in the matrix notation as

$$d\sigma_\alpha = H''_{\alpha\beta}\, d\epsilon_\beta \text{ where } \alpha, \beta, = 1 \text{ to } 6 \tag{B.1}$$

$$\text{Let us define } a \equiv \frac{2G^2}{(M + 2G)J'_2} \tag{B.2}$$

Instead of evaluating all the components of the H'' matrix, we have calculated the matrix components relevant to our problem. In our work we are restricted to plane strain loading and only the principal stresses and strains are of interest. The pertinent components of the matrix H'' are given as

$$H_{11} = K + \frac{4}{3}G - \frac{1}{3}a\sigma'_{11}\,(2\sigma'_{11} - \sigma'_{22} - \sigma'_{33})$$

$$H_{12} = K - \frac{2}{3}G - \frac{1}{3}a\sigma'_{11}\,(-\sigma'_{11} + 2\sigma'_{22} - \sigma'_{33})$$

$$H_{13} = K - \frac{2}{3}G - \frac{1}{3}a\sigma'_{11}\,(-\sigma'_{11} - \sigma'_{22} + 2\sigma'_{33})$$

$$H_{21} = K - \frac{2}{3}G - \frac{1}{3}a\sigma'_{22}\,(2\sigma'_{11} - \sigma'_{22} - \sigma'_{33})$$

$$H_{22} = K + \frac{4G}{3} - \frac{1}{3}a\sigma'_{22}\,(-\sigma'_{11} + 2\sigma'_{22} - \sigma'_{33})$$

$$H_{23} = K - \frac{2G}{3} - \frac{1}{3}a\sigma'_{22}\,(-\sigma'_{11} - \sigma'_{22} + 2\sigma'_{33})$$

$$H_{31} = K - \frac{2G}{3} - \frac{1}{3}a\sigma'_{33}\,(2\sigma'_{11} - \sigma'_{22} - \sigma'_{33})$$

$$H_{32} = K - \frac{2}{3}G - \frac{1}{3}a\sigma'_{33}\,(-\sigma'_{11} + 2\sigma'_{22} - \sigma'_{33})$$

$$H_{33} = K + \frac{4}{3}G - \frac{1}{3}a\sigma'_{33}\,(-\sigma'_{11} - \sigma'_{22} + 2\sigma'_{33})$$

APPENDIX C

Evaluation of $d\gamma^p$

In our work we have defined γ^p as

$$\gamma^p = \sqrt{I_2'^p} = \left(\frac{1}{2}\epsilon'^p_{ij} \cdot \epsilon'^p_{ij}\right)^{1/2} \tag{C.1}$$

This can be written as

$$\gamma^p = \left[\frac{1}{2} \int d\epsilon'^p_{ij} \int d\epsilon'^p_{ij}\right]^{1/2} \tag{C.2}$$

Using Equations (9) and (12) in Section II, we can write

$$\gamma^p = \left[\frac{1}{2} \int d\lambda \frac{\sigma'_{ij}}{2\sqrt{J'_2}} \int \frac{d\lambda}{2\sqrt{J'_2}} \sigma'_{ij}\right]^{1/2} \tag{C.3}$$

For proportional loading, we can write[15]

$$\sigma'_{ij} = \beta_{ij}\sqrt{J'_2} \text{ where } \left(\frac{1}{2}\beta_{ij}\beta_{ij}\right)^{1/2} = 1 \tag{C.4}$$

Using these relations we can write

$$\gamma^p = \left[\frac{1}{2} \int \frac{d\lambda}{2}\beta_{ij} \int \frac{d\lambda}{2}\beta_{ij}\right]^{1/2} = \int \frac{d\lambda}{2} \tag{C.5}$$

Upon differentiating, we get the required result

$$d\gamma^p = \frac{d\lambda}{2} \tag{C.6}$$

A detailed discussion of this derivation can be seen in Appendix C of Reference 15.

TABLE I

Material Constants for Ytterbium Foils[a]

Resistivity	38-43$\mu\Omega$ - cm
Bulk Modulus	148 kbar
Young's Modulus	120 kbar
Yield Stress in Simple Tension (0.2% offset)	0.82 kbar
Strain Hardening Coefficient	3.04 kbar[b]
Piezoresistive Coefficient, π_{11}	-4.2×10^{-2} kbar^{-1}
Piezoresistive Coefficient, π_{12}	-7.88×10^{-3} kbar^{-1}
Electrical Strain Hardening Coefficient, η	1.13

[a] Values taken from Reference 9. Some of the values presented here have been modified in the present work. See Section IV.B for explanation.

[b] The strain hardening coefficient given in Reference 9 was converted for use in the multi-dimensional loading encountered in the present work. See discussion following Eq. (8) in Reference 9.

TABLE II: Determination of η from Residual Resistance[a]

Experiment Number	Peak Stress (kbar)	Plastic Strain (γ^p) Upon Unloading	Calculated[b] $\left.\frac{\Delta R}{R_o}\right\|_{\eta = 0}$	Measured $\frac{\Delta R}{R_o}$	η
1	1.25	5.13×10^{-4}	3.07×10^{-3}	0.01	13.5
2	1.85	3.03×10^{-3}	1.81×10^{-2}	0.033	4.9
3	3.6	1.5×10^{-2}	3.11×10^{-2}	0.06	1.9
4	5.4	2.92×10^{-2}	3.74×10^{-2}	0.076	1.3
5	6.5	3.84×10^{-2}	3.39×10^{-2}	0.09	1.5
6[c]	7.4	4.54×10^{-2}	3.84×10^{-2}	0.12	1.8

[a] These results are valid for the particular batch of foils used in this work.

[b] These values are the result of the residual stresses and strains in the foils.

[c] The η value for this experiment is suspect because the effect of matrix inelasticity is showing up. See text.

FIGURE CAPTIONS

Figure 1. Typical resistance-change versus time profile from a shocked ytterbium gauge. This record is for a peak stress of 11.6 kbar in the matrix.

Figure 2. The residual resistance change for the two gauge orientations versus peak longitudinal matrix stress. In region I, the matrix and gauge remain elastic. In region II, the gauge deforms inelastically but the matrix is elastic. In region III, both the gauge and matrix deform inelastically.

Figure 3. Experimentally determined electrical strain-hardening coefficient, η, versus plastic strain in the gauge foil.

Figure 4. Peak resistance change for the two orientations as a function of peak longitudinal stress in the matrix (shock data). The points are the experimental data and the lines represent model predictions. Above the threshold for inelastic deformation in PMMA, the calculation is shown as a broken line. See text for full explanation.

Figure 5. Resistance change for the two orientations as a function of longitudinal matrix stress (quasi-static experiments). The points represent the data and the lines represent model predictions.

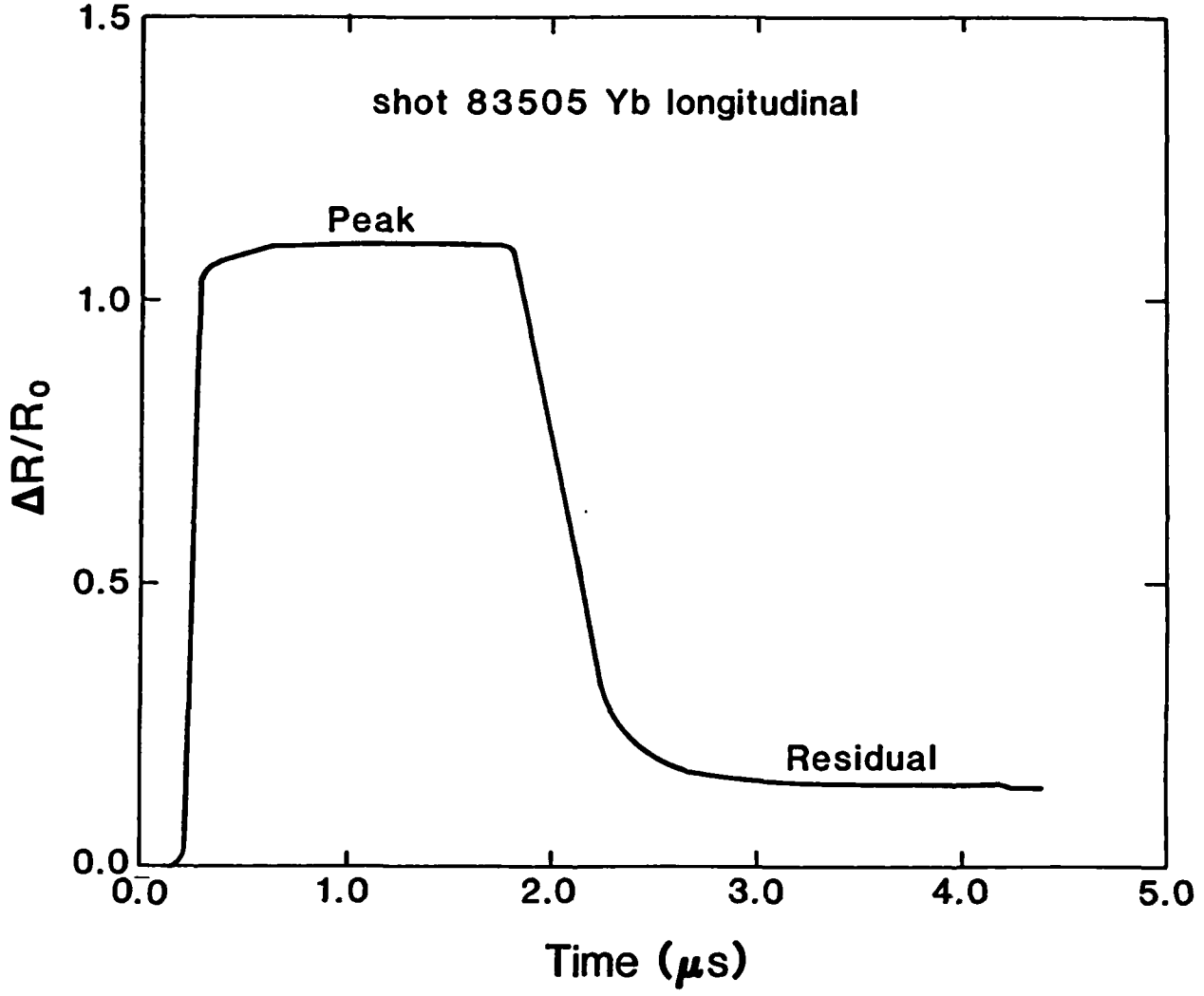

Figure 1 Cmpsta & Cmbsta

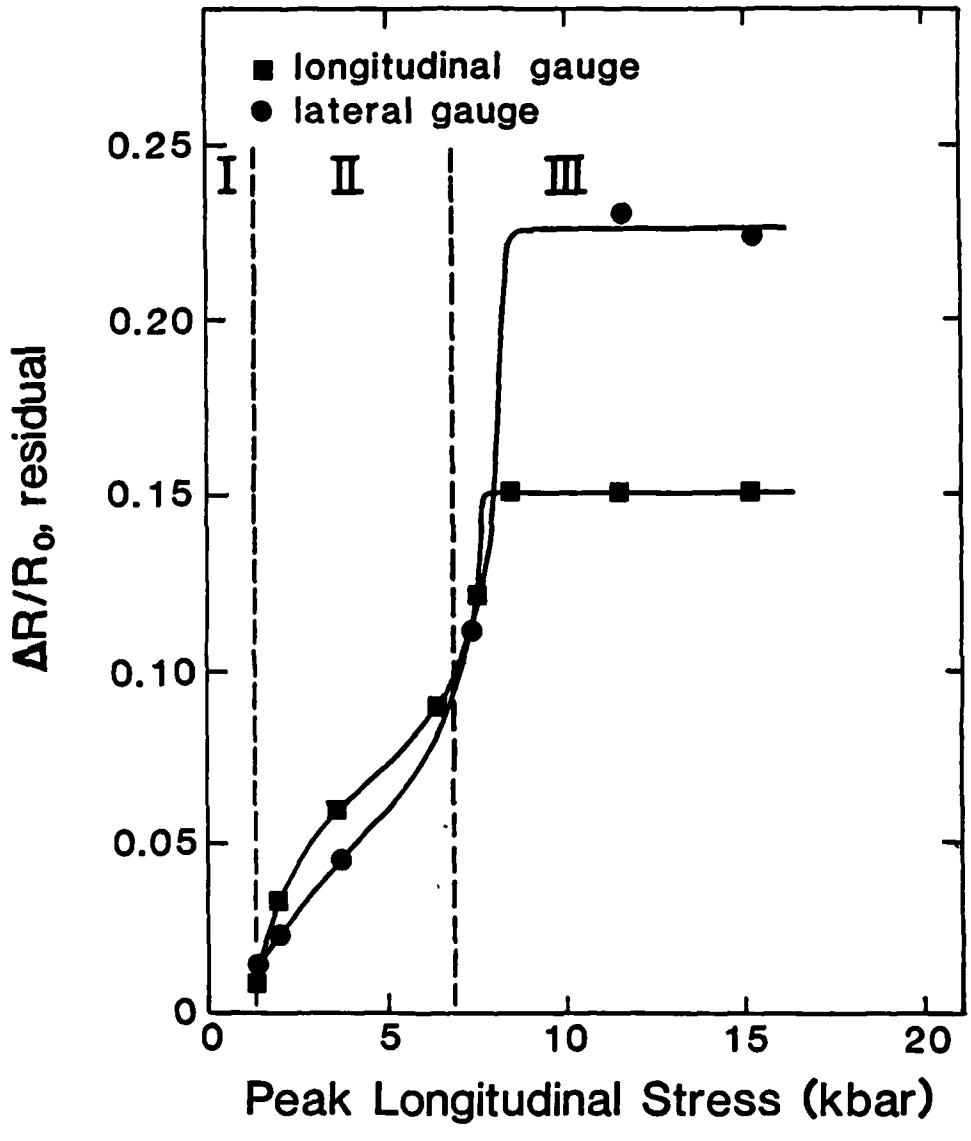

Figure 2 Gupta & Gupta

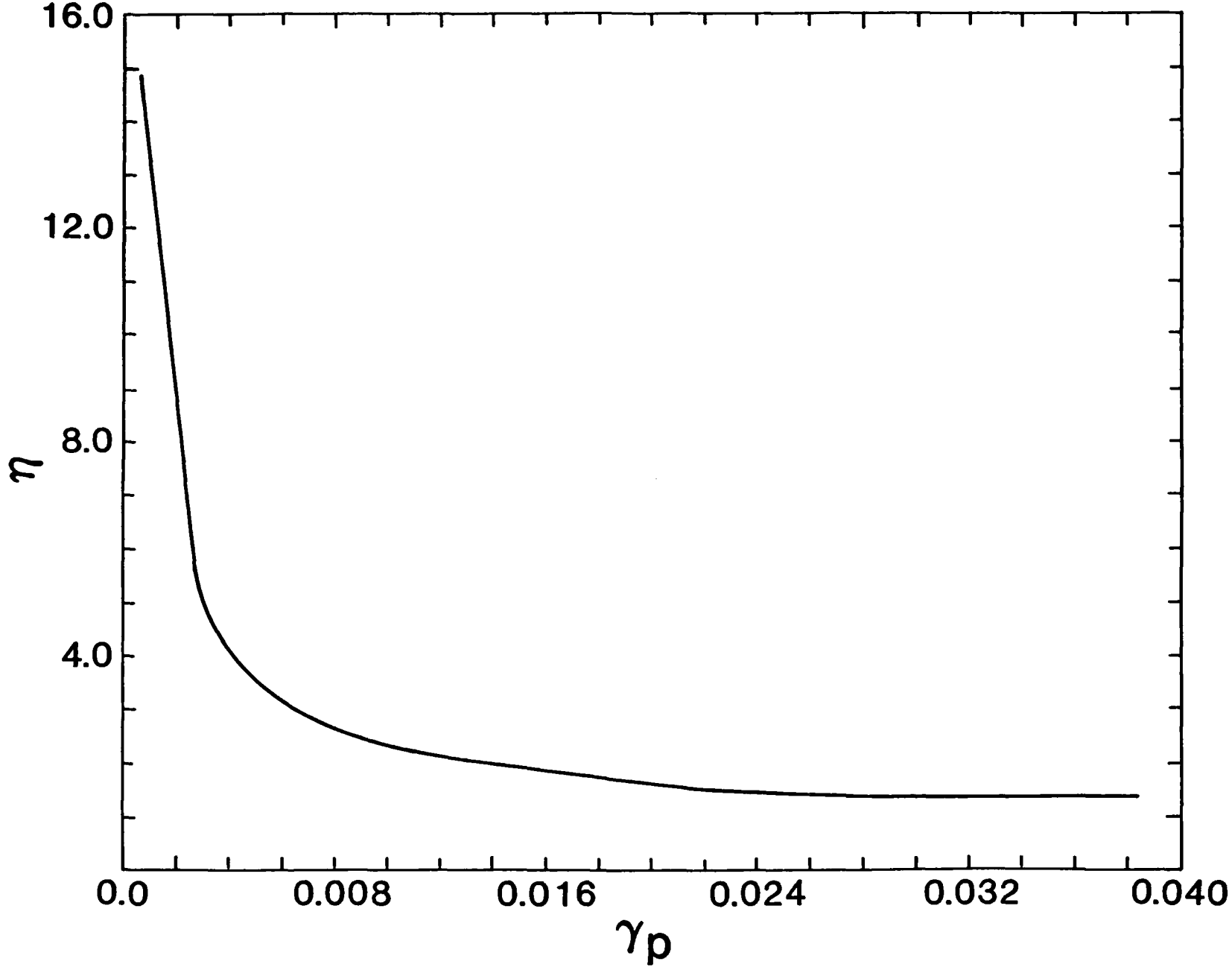

Figure 3 Gupta & Gupta

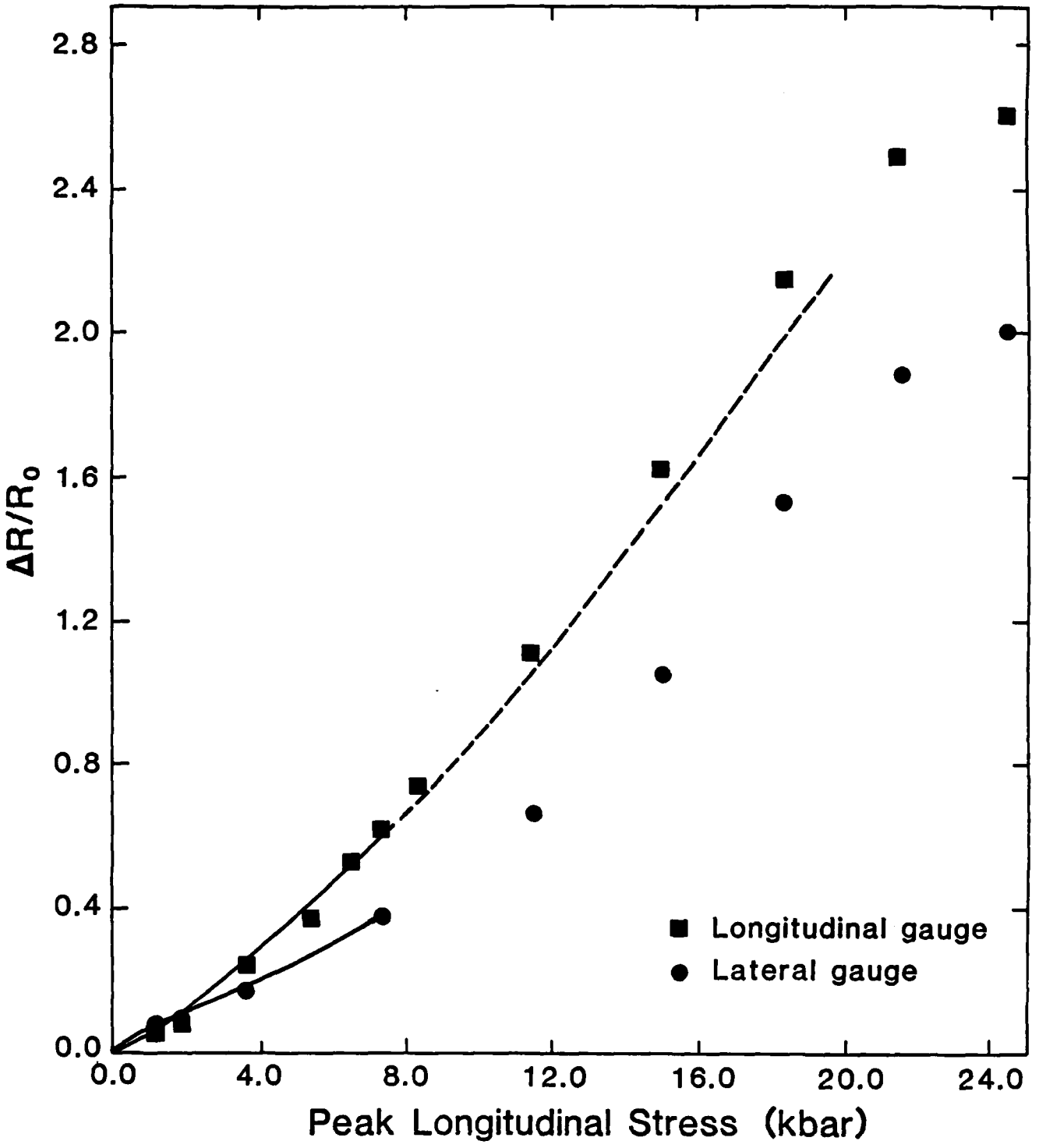
2.8
2.4
2.0
1.6
1.2
0.8
0.4
0.0
ΔR/R₀
0.0
4.0
8.0
12.0
16.0
20.0
24.0
Peak Longitudinal Stress (kbar)
Longitudinal gauge
Lateral gauge

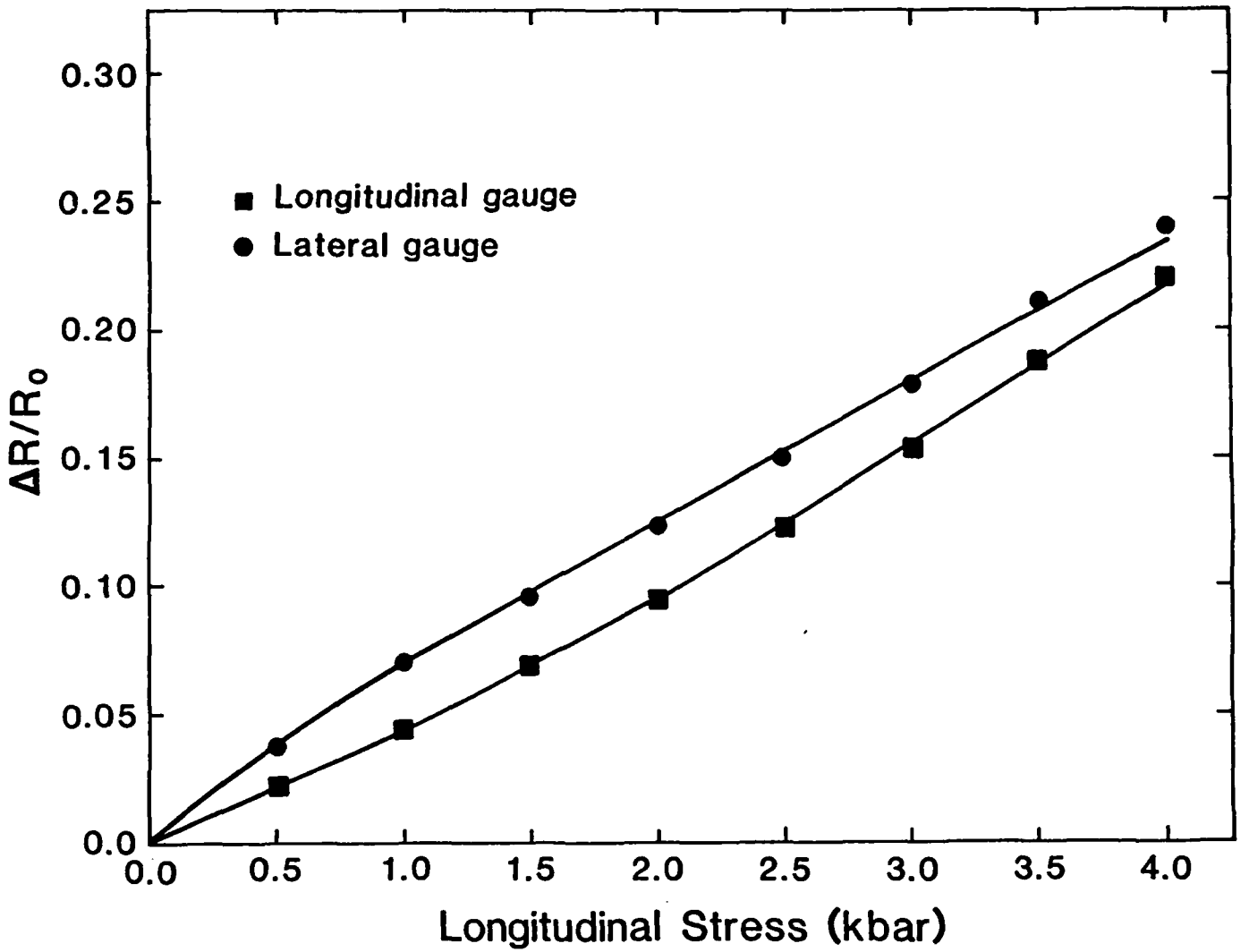

Figure 5 Cu pts & Cu pts

APPENDIX 2

PIEZORESISTANCE RESPONSE OF YTTERBIUM FOIL GAUGES SHOCKED TO 45 KBAR IN FUSED SILICA MATRIX

N. S. Brar* and Y.M. Gupta

Shock Dynamics Laboratory

Department of Physics

Washington State University

Pullman, WA 99164-2814

ABSTRACT

Resistance change at peak stress and the residual resistance change of ytterbium foil gauges embedded at different depths in fused silica matrix were determined under shock loading to a matrix stress of 45 kbar. The results show that for a given peak stress, the gauge response was unchanged for an order of magnitude variation (10^3 - 10^4 kbar/μs) in the loading rate. Measured resistance change at peak stress and upon unloading agree very well with the analytic model calculations for matrix stresses up to 30 kbar. Peak resistance change values in the present work have been reconciled with earlier ytterbium data in PMMA matrix on the basis of differences in longitudinal stress in the gauge foils for the two matrix materials and differences in the electromechanical constants of the two sets of foils. Above 30 kbar matrix stress, measured resistance values are lower than the calculated values. This difference is attributed to changes in the ytterbium as a result of the initiation of the FCC to BCC phase transition. The resistance change-time profile from the 45 kbar experiment shows a strongly time-dependent behavior suggesting that a significant fraction of the material has been transformed.

* Present address: Impact Physics Laboratory, University of Dayton Research Institute, Dayton, Ohio.

I. INTRODUCTION

The present work is a part of an on going effort to develop a detailed understanding of the dynamic response of piezoresistance gauges.[1-6] The impetus for the investigation has been the phenomenological model developed by Gupta for interpreting piezoresistance measurements.[3] Recently, a comprehensive set of shock wave experiments have been performed to determine the response to 25 kbar of ytterbium foil gauges for two different orientation in a PMMA matrix.[5] To analyze these results quantitatively, particularly the residual resistance change data, the inclusion analysis described in Reference 3 was extended to incorporate strain-hardening.[6] Over the elastic range of the PMMA (approximately 7.5 kbar), good agreement was observed between the calculations and experimental measurements for both gauge orientations.[6] Beyond 7.5 kbar, the agreement between theory and experiment was quite good for the longitudinal gauge up to 20 kbar. The lateral gauge response, over this stress range, could not be analyzed because the PMMA constitutive response is not well understood beyond 7.5 kbar.[7] Two results in the earlier work on ytterbium that have been speculated on, but not completely understood,[5,6] are: the change in the slope of the resistance change versus stress curve at approximately 20 kbar; the rapid increase in the slope of the residual resistance versus stress curve around 7-8 kbar matrix stress. Both of these issues are important for using ytterbium gauges to make time-resolved measurements under shock loading.

The work presented in this paper had the following objectives: (i) to ascertain the effects of loading rate, if any, on the gauge response, (ii) to measure and quantitatively analyze the response of ytterbium gauges to 40 kbar by performing experiments in a well characterized elastic matrix, (iii) to develop a detailed understanding of the gauge hysteresis or residual resistance over the entire stress range of interest, and (iv) to compare the present results with the earlier work in the PMMA matrix to resolve the issues indicated above.

We chose fused silica as the matrix material for our experiments, because of the following characteristics:[7] it has been well characterized under shock loading conditions; ramp waves are generated in fused silica because of its anomalous compression and the rise time of the ramp wave at

a point in the matrix is a function of its position with respect to the impact surface and the impact stress; and it stays elastic to matrix stresses of about 90 kbar. The ramp wave property of fused silica is appropriate for studying the loading rate effects on the gauge response. Two gauges embedded at different depths in the matrix will be loaded at different rates to the same peak stress. The elastic response of fused silica permits us to quantitatively analyze the experimental results at matrix stresses well in excess of 7-8 kbar, and to understand the PMMA results by making comparison with the earlier results.

II. EXPERIMENTAL METHOD

A. Material Characterization

Ytterbium foils with a nominal thickness of 50 μm were obtained from Research Chemical Corporation, Phoenix, Arizona. These foils were characterized in terms of their electromechanical constants by performing quasistatic experiments following the method developed by Chen, *et al.* [4] The electromechanical constants of the present batch of foils and comparisons with the previous batch of foils used in the earlier experiments[5] are presented in Reference 8. It was found that mechanical constants of the two batches of foils were significantly different, but the linear piezoresistive constants of the two batches were almost identical. Hence, direct quantitative comparisons between the resistance change results of the present batch of foils with those used in earlier experiments[5] are difficult. Instead, a discussion based on the trends in the experimental data and on an analysis of the results will be presented. For completeness, the material constants for the foils used in the present work are summarized in Table I. The fused silica used in our experiments was Dynasil 1000[10] and was obtained from Adolf Meller Co.

B. Dynamic Experiments

Ten experiments, with the longitudinal matrix stress ranging between 2.8 and 45 kbar, were performed. Fused silica targets, containing two gauges in the longitudinal orientation, were

assembled as shown schematically in Fig. 1. Gauges G1 and G2 were at depths of 1 mm and 7.35 mm ,respectively, from the impact surface of the target.[11] The intent was to load the two gauges to the same peak stress but at different loading rates. Ytterbium gauges were cut to facilitate four terminal resistance measurements.[5] Copper leads, 0.001" thick, were soldered to the gauge leads to make connections with current and voltage cables. Gauges were embedded into grooves of nearly matching dimensions, using very thin layers of hysol epoxy. A 1 mm thick fused silica disc was bonded on to the 6.53 mm thick disc to cover gauge G1. This target design worked well for the experiments to peak stresses of 25 kbar. In experiments at 30 and 35 kbar we found that the record from gauge G2 was very noisy, due to reasons that are not entirely clear.[12] This problem was overcome by repeating the experiment at 35 kbar with a target containing only one gauge, G2. The gauge was emplaced into a groove on a 9.53 mm thick fused silica disc and was covered by gluing a 6.35 mm fused silica disc on top of the 9.53 mm thick disc. The record from gauge G2 in this experiment was of very good quality. The experiment at 39.6 kbar was also performed with only gauge G2 in the target. The target for the experiment at the highest stress of 45 kbar was assembled with one ytterbium and one manganin gauge on the same plane. This was done to obtain an independent measure of the stress in the matrix using the manganin gauge output.

The experiments were performed using the 6.35 cm gas gun at our laboratory. For the experiment at a stress of 2.8 kbar, PMMA (Rohm and Haas Type II UVA),[7] served as the impactor material. The experiments between 9.4 and 39.6 kbar were performed using fused silica impactors. The impactor thickness in each of these experiments was appropriate to obtain complete unloading of the matrix while it was in a state of uniaxial strain. The experiment at 45 kbar was performed with a z-cut sapphire impactor.[7] Because of the high mechanical impedance of z-cut sapphire relative to that of fused silica, complete unloading of the matrix did not take place during the time duration for uniaxial strain in this experiment.

Although the electrical circuit used for recording the resistance change, $\Delta R/R_o$, of the gauge was similar to that reported in Reference 5, a circuit analysis showed that at the highest resistance

change of interest in our experiments the measured voltage change, $\Delta V/V_o$, differed from $\Delta R/R_o$ by approximately 3 percent. Using the procedure outlined in Keough's report,[13] a correction for this difference was made in our work. The difference of 1 percent cited in Reference 5 is incorrect because the resistance change in the gauge leads was not incorporated into the analysis.

III. EXPERIMENTAL RESULTS

A typical profile of resistance change versus time is shown in Fig. 2; this record is from gauge G2 for a peak matrix stress of 25 kbar. The almost flat top of the profile from 0.23 to 1.4 μsec corresponds to a resistance change of 2.6 at the peak stress. The average residual resistance change value from the point of complete unloading at 1.4 μsec to 2.0 μsec where the gauge leads failed was determined to be 0.14. Data from nine of the ten experiments are summarized in Table II; the 45 kbar datum is discussed later. The resistance change vs time profiles from gauges G1 and G2 in experiments 1-5 were essentially similar to the profile shown in Fig. 2. In experiments 6 and 7, residual resistance data, due to lead breaking, were not obtained. Also the profiles from gauges G2 in these two experiments were noisy and the resistance changes at the peak stresses were lower than those from gauges G1 in each case. In experiment 8 (repeat of 7) with only one gauge, G2, the resistance change at the peak stress of 35 kbar was comparable to that from G1 in experiment 7. But the residual resistance change data again were not obtained. Apparently the gauge leads failed prematurely in all three of these experiments. We solved this problem of lead failure by replacing the 0.001" thick copper leads with 0.004" thick leads and by making the impactor size smaller than that of the target. This experimental design worked well in experiment 9 at 39.6 kbar matrix stress, and we obtained the complete resistance change profile, including the residual resistance change.

In experiment 10, at 45 kbar matrix stress, the response of the ytterbium gauge, as shown in Fig. 3, was strongly time dependent. The resistance change profile of the manganin gauge from this experiment, included in Fig. 3, showed that the fused silica matrix response was elastic as expected.[7] The 45 kbar stress inferred from the manganin gauge calibration[14] agreed with the calculated valuc

from the z-cut sapphire and fused silica Hugoniots.[7] Thus, the time-dependent response of ytterbium represents a real change in the ytterbium properties as discussed later.

The resistance change values corresponding to the peak stress, $(\Delta R/R_o)_{peak}$, and the residual resistance change values, $(\Delta R/R_o)_{residual}$, are plotted as a function of the matrix longitudinal stress in Figures 4 and 5, respectively. Results of the analytical calculations, discussed in the next section, are also shown in these figures.

IV. ANALYSIS AND DISCUSSION

A. Loading Rate Effects

As indicated in Section I, the location of gauges G1 and G2 in the fused silica target with respect to the impact surface determined the loading rate at the gauge locations. For example, at a peak stress of 25 kbar, the loading rates for G1 and G2 were 0.961 kb/nsec and 0.131 kb/nsec, respectively.[7] Loading rate effects on the gauge response would show up as a systematic variation between resistance change values for the two gauges. Comparison of the data from the two gauges in Figure 4 shows good agreement within experimental scatter and rules out loading rate effects (within this range) on the gauge response. This result is important because it demonstrates that for an arbitrary wave shape, encountered in most problems of interest, the measured resistance change values can be analyzed using calibrations obtained from step loading experiments.

B. *Comparison of Calculated and Measured Response to a Peak Stress of 30 kbar.*

The resistance change profile shown in Figure 2 is typical of the profiles observed in our experiments. Hence, we have chosen to calculate the resistance change at the peak stress and the residual change value for different matrix stresses. These calculations were performed using the calculational method described in earlier papers.[3,6] Using the nomenclature presented in the earlier papers, only the main features of the calculations are summarized here. Details may be seen in References 3 and 6.

The equation for calculating the resistance change is:

$$\frac{\Delta R_z}{R_o} = \Pi_{12}(\Delta\sigma_x + \Delta\sigma_y) + \Pi_{11}\Delta\sigma_z + \Delta\epsilon_z - \Delta\epsilon_x - \Delta\epsilon_y + \eta\Delta\epsilon^p \qquad (1)$$

where x,y, and z are the axes along the gauge width, thickness, and length, respectively: the stresses (σ) and the strains (ϵ) refer to stresses and strains in the gauge; ϵ^p is a scalar measure of plastic strain in the gauge; Π_{11} and Π_{12} are piezoresistive coefficients and η is the electrical strain hardening

coefficient. The various material constants (mechanical and electromechanical) were measured for the present batch of foils[8] and are summarized in Table I. The specific steps for determining $\Delta R_z/R_o$ in Eq. (1) are as follows:

(i) The stresses (σ), strains (ϵ), and the plastic strain (ϵ^p) in the gauge corresponding to the peak stress and unloading in the fused silica matrix were determined from the inclusion analysis.[6] Details of these calculations that are specific to the fused silica matrix are described in the Appendix.

(ii) Upon unloading in the fused silica, the residual stresses in the gauge are non-zero but are small enough to neglect the pressure dependence of the piezoresistive coefficients. Using the linear piezoresistive coefficients measured for the present batch of foils (see Table I) and the residual stresses and strains calculated in the gauge in step (i), the $\eta\epsilon^p$ contribution to the residual resistance change was determined from Eq. (1). From the calculated value of ϵ^p, a smooth, monotonically decreasing curve was drawn to represent η as a function of ϵ^p. This curve is similar, but not identical, to the curve shown in Reference 6; the two sets of foils came from different batches. This functional relationship can then be used to to obtain η as needed in the resistance change calculation in Equation (1) for a given matrix compression.

(iii) The variation of the piezoresistive coefficients, Π_{11} and Π_{12} with pressure was assumed to be linear[6]:

$$\Pi_{11} = \Pi_{11}^{o} + mP$$
$$\Pi_{12} = \Pi_{12}^{o} + mP$$

where the subscript o indicates zero pressure values and P is defined to be the mean compressive stress ($-\sigma_{mm}/3$). For m, we have used the value (7.6×10^{-4} kbar $^{-2}$) derived in the earlier work on ytterbium in a PMMA matrix.[6]

Using the steps indicated above, the resistance change values as a function of the peak longitudinal stress in the matrix have been plotted in Figure 4. The measured resistance change data from gauges G1 and G2 for matrix stresses to 30 kbar agree very well, within experimental error, with the calculated curve. This good agreement demonstrates the adequacy of the theoretical model to predict the resistance change of ytterbium gauges embedded in an elastic matrix. Above 30 kbar the agreement between the calculations and measurements is not good. This behavior is similar to that observed above 20 kbar in a PMMA matrix and is discussed later in this section.

C. Residual Resistance Change

An important aspect of the present work is a detailed examination of the residual resistance values measured in the experiments. Because the matrix stays elastic over the entire stress range of the experiments, the residual resistance change data can be analyzed quantitatively over a wider range of stresses than the data obtained in a PMMA matrix.[6] Using the procedure indicated in step (ii), contributions from the residual stresses and strains in the gauge foil, and from the increase in resistivity due to plastic strain (generation of defects in the lattice) can be separated. In Table III, the measured and calculated residual values for various peak stresses are shown; these results along with the measurements in the PMMA matrix[5] are plotted in Figure 5. Comparisons with the PMMA results will be discussed in the next sub-section.

Overall, the agreement between the calculations and the experiments is quite good and lends confidence to using the calculations to understand the residual resistance response of the gauge foils. The maximum peak matrix stress at which no residual resistance change is predicted from our analytic model is 1.5 kbar as shown in Figure 5. This value corresponds to the threshold stress for the ytterbium to undergo plastic deformation as pointed out in Reference 3. For peak matrix stresses above this value, the ytterbium undergoes plastic contribution and provides two distinct contributions to the residual resistance[6]: residual stresses and strains in the gauge foil even though the matrix far away from the foil has no stresses and strains, and the increase in the resistivity ($\eta\epsilon^p$). In Table III,

the relative magnitude of these two contributions is indicated. Because of the large piezoresistive coefficients of ytterbium, the first term tends to dominate over the entire stress range of interest. The near-parabolic form of the curve for the fused silica matrix in Figure 5, is a consequence of the approach to saturation expected for the foil in an elastic matrix.[6] The present results provide confirmation of an earlier conclusion that the calculation of residual stresses and strains (inclusion problem) in the gauge foil is important for a detailed analyses of the gauge response.[3] More general discussion about residual resistance change and gauge hysteresis may be seen in Reference 6.

Although the overall comparison in Figure 5 is quite good, the comparisons at 2.8 and 9.4 kbar between the measurements and calculations are not as good. For these low stresses the magnitude of the measured and calculated quantities are very small, and consequently they have large relative errors. At 39.6 kbar matrix stress the measured and calculated residual resistance change agree very well. This is surprising because the measured peak resistance change for this matrix was found to be considerably lower than the calculated value (Figure 4). As discussed later, we believe that ytterbium undergoes a change in its physical properties above a matrix stress of 30 kbar. The good agreement between the calculated and measured residual resistance, however, suggests that any changes in the physical properties that might have taken place at the peak stress are recovered upon unloading. Hence, the calculated residual resistance change agrees with the measured residual resistance change. More data are needed to confirm this conjecture.

D. Gauge Response Above a Peak Stress of 30 kbar

Above 30 kbar peak stress, the measured resistance change is lower than the calculated values shown in Figure 4. This discrepancy increases with increasing stress, and eventually at 45 kbar, the strongly time-dependent behavior shown in Figure 3 is observed. Previous work on fused silica[7] and the manganin response in Figure 3 confirm that the observed time-dependent response is a property of the ytterbium. The large decrease in the resistance and the stress at which it occurs suggests that the ytterbium is undergoing the FCC→BCC phase transition observed in static high pressure

studies.[15–17] It appears that the 30 kbar value represents the onset of the transition and results in a change in the physical properties of the ytterbium. The material constants in the calculations are based entirely on Phase I properties of the ytterbium. Hence, the discrepancy in the measurements and the calculations above 30 kbar.

E. Comparison of the Gauge Response in Fused Silica and in PMMA.

As indicated in Section II, the ytterbium foils used in the present work are from a different batch than those used in the PMMA work earlier in Reference 5. Therefore, comparisons between the two sets of data have to be in terms of important qualitative trends or using analyses that take into account the differences in material properties of the batches of foils. In a separate study[8] we have compared the results from the two foil batches for the same matrix (PMMA) and shown that batch I (used in Reference 5) gave somewhat higher resistance change values than batch II (used in the present work). The measured differences were similar to the differences predicted by the analytical calculations performed using the appropriate material constants.

In Figure 6, the peak resistance change data as a function of longitudinal matrix stress are plotted from the present work and Reference 5. Smooth curves are drawn to fit the two sets of data; up to 20 kbar, the $\Delta R/R_o$ values from the PMMA experiments lie above the values from the fused silica experiments. This difference is due to two factors: the differences in foil batches indicated above and the differences in the longitudinal stress in the gauge foils for the two matrix materials. In Reference 18 it has been shown that the longitudinal stress in the foil is lower than the longitudinal stress in the matrix if the mechanical impedance of the matrix is higher than the mechanical impedance of the foil. For fused silica and ytterbium, the difference in mechanical impedances is small, but does lead to an observable stress difference, e.g. for 20.3 kbar in the matrix the stress in the foil is 19.0 kbar. This effect is a consequence of the "inclusion problem" and is taken into account in our calculations shown in Figure 4. In contrast to the fused silica matrix, the PMMA

matrix has a lower mechanical impedance than ytterbium and the longitudinal stress in the two is the same.[18]

When the two differences indicated above are accounted for by using the analytic model, the two sets of data are very close up to 20 kbar. Beyond 20 kbar, there are differences that are not related to factors indicated above. Both sets of data in Figure 6 shown a flattening of the curves or distinct changes in slope. For PMMA it occurs above 20 kbar, and for fused silica it occurs above 30 kbar. These changes in the slope raise the following questions: (i) What is the physical mechanism causing this change in slope and is it the same in the two matrix materials? (ii) If the mechanism is the same, then why does it occur at such different stresses in the two materials. The answers to these questions are important for gaining a fundamental understanding of shock compressed ytterbium and for determining the stress range over which these gauges can be used in materials of interest.

Without a detailed study it is difficult to answer these questions. In Reference 5, it was conjectured that the change in slope above 20 kbar may be a precursor to the FCC→BCC phase transition reported at 40 kbar in static high pressure studies.[15–17] The present data above 30 kbar, discussed earlier, support the occurrence of this transition in the fused silica experiments. However, the present results do not provide sufficient information to explain the results observed in PMMA. As indicated in Reference 5, it is likely that the details of the transition will depend on the stress and strain states in the foils which in turn are related to the matrix properties. Further experiments are needed to resolve this issue.

The measured residual resistance change data for the two matrix materials are shown in Figure 5. The data in fused silica, discussed earlier, show a near-parabolic increase to the highest matrix stress and good agreement with the calculations. In contrast, the data in PMMA show a large increase in the slope around a matrix stress of 7.5 kbar. Up to this stress value in PMMA, the measurements and calculations matched quite well.[6] The increase in the slope of 7.5 kbar was ascribed to the onset of inelastic deformation in the PMMA matrix[6] and calculations beyond this value were not possible without a knowledge of the PMMA constitutive model. Comparisons of the

earlier results with the present results in the fused silica matrix support the hypothesis of inelastic deformation in the PMMA matrix. The inelastic deformation of the matrix would result in residual stresses and strains in the matrix upon unloading[7] and the effect would be most pronounced near the threshold stress in the matrix. At higher stresses, the residual stresses in the matrix would tend towards saturation. The absence of a sudden change in the fused silica data suggests that the results in PMMA are due to the matrix residual stresses and strains and lend credibility to the interpretation presented for the PMMA matrix. Finally, these results demonstrate the possibility of using in-groove gauges to measure residual stresses in materials of interest.

V. Summary

The main conclusions from the present work can be summarized as follows:

1. The response of ytterbium gauges, as determined by the measured resistance changes, is found to be independent of the loading rate over the range (10^3 – 10^4 kbar/μs) examined here.

2. The peak resistance change values predicted from the analytical model are in very good agreement with the experimental measurements up to a matrix longitudinal stress of 30 kbar. Above 30 kbar, the measured resistance change is lower than the calculated values. This stress value appears to mark the onset of the FCC→BCC transition in shocked ytterbium.

3. The measured and calculated residual resistance values are in good agreement over the entire stress range of interest. The residual resistance change values are dominated by contributions from residual stresses and strains caused by inelastic deformation of the foils, the permanent change in resistivity due to generation of lattice defects has a smaller contribution.

4. Above 30 kbar, the difference between measured and calculated resistance change values increases. The datum at 45 kbar shows a strongly time dependent response suggesting that a significant fraction of the ytterbium has been transformed. We conjecture that the

transformation starts at 30 kbar and the amount of the transformed material increases with stress. Hence, the increasing discrepancy between the model predictions (based on Phase I constants) and the experimental results. The agreement between the residual resistance value at 39.6 kbar suggests that almost all of Phase I material is recovered upon unloading.

5. Present data on residual resistance change in an elastic matrix have been helpful in separating gauge and matrix contribution to residual resistance measurements in a PMMA matrix.[5] Comparison of data for the two matrix materials suggests that the sharp increase observed in the residual resistance at 7.5 kbar in PMMA is due to the inelastic deformation of the PMMA matrix.

6. Present data on peak resistance change values can be quantitatively reconciled with the earlier ytterbium data reported for a PMMA matrix below 20 kbar[5] on the basis of the differences in the eletromechanical constants of the foil batches and the differences in the longitudinal stress in the gauge foils.

The present work, coupled with earlier studies,[4–6,8] has provided a comprehensive understanding of the piezoresistance response of ytterbium foils under shock loading including an understanding of gauge hysteresis or residual resistance. The one problem that requires further examination is a reconciliation of the ytterbium response above 20 kbar in PMMA and above 30 kbar in fused silica. We believe that these two sets of data are manifestations of the ytterbium transformation under different conditions. This aspect of the ytterbium response under shock loading is currently being studied and will be reported in a subsequent publication.

ACKNOWLEDGMENTS

Jerry Thompson is sincerly thanked for his help with the experimental effort. This work was supported by AFOSR Grant 82-0132.

REFERENCES

1. Y.M. Gupta, D.D. Keough, D. Henley, and D.F. Walter, Appl. Phys. Lett. 37:395 (1980).
2. Y.M. Gupta, J. Appl. Phys. 54:6094 (1983).
3. Y.M. Gupta, J. Appl. Phys. 54:6256 (1983).
4. D.Y. Chen, Y.M. Gupta, and M.H. Miles, J. Appl. Phys. 55:3984 (1984).
5. S.C. Gupta and Y.M. Gupta, J. Appl. Phys. 57:2464 (1985).
6. Y.M. Gupta and S.C. Gupta, "Incorporation of Strain-Hardening in Piezoresistance Analysis: Application to Ytterbium Foils in a PMMA Matrix", submitted to J. Appl. Phys.
7. L.M. Barker and R.E. Hollenbach, J. Appl. Phys. 41:4208 (1970).
8. N.S. Brar and Y.M. Gupta, in Shock Waves in Condensed Matter, p. 513, Edited by Y.M. Gupta (Plenum Publishing, N.Y.) 1986; Bull. Amer. Phys. Soc. 30, 1311 (1985).
9. D.E. Grady and M.J. Ginsberg, J. Appl. Phys 48:2179 (1977).
10. This material is intended to be a replacement for GE Type 151 fused silica that was exmined in Ref. 7.
11. In our experiments there is no difference between the terms gauges and foils, and the two words are used synonymously.
12. We conjecture that at these high impact stresses the presence of gauge G1 may cause local failure of the material and thereby modify the amplitude and shape of the stress pulse to a significant extent.
13. D.D. Keough," Procedure for Fabrication and Operation of Manganin Shock Pressure Gauges", Technical Report No. AFWL-TR-69-57, Contract No. AF29(601)-68-C-0038, SRI International, Menlo Park, CA. (1970) (unpublished).

14. S.C. Gupta and Y.M. Gupta, in Shock Waves in Condensed Matter, p. 509, Edited by Y.M. Gupta (Plenum Publishing, N.Y.), 1986; Bull. Amer. Phys. Soc. 30, 1311 (1985)

15. A. Jayaraman, Phys. Rev. 35:A1056 (1964).

16. H.T. Hall and L. Merrill, Inorg. Chem. 2:618 (1963).

17. P.C. Souers and G. Jura, Science 140:481 (1963).

18. S.C. Gupta and Y.M. Gupta, Bull. Amer. Phys. Soc. 29:741 (1984); full text is currently under preparation.

APPENDIX

Inclusion Calculations in Fused Silica

A discussion of the matrix loading and unloading moduli for the inclusion calculation has been presented in Reference 6. Here, we indicate the procedure used to specify the bulk and shear moduli (K & G) for fused silica as needed for our inclusion calculations. Using the stress-strain relation under shock loading[7], we can determine the strain values corresponding to different peak stresses in the fused silica. Using a straight line between the initial and final states, the loading modulus, K_L, pertaining to a particular experiment can be determined. For a normal material, this amounts to loading along the Rayleigh line. Using the ultrasonic shear wave velocities indicated for fused silica[7], the loading modulus $\left[K_L = K + \frac{4}{3}G\right]$ was divided into K and G values. These values were then used in our calculations. The unloading calculations were carried out using the same values of K and G as for loading.

The procedure we have used is not rigorously correct for loading because the fused silica has an anamalous compression curve. However, the final solution is not very sensitive to the actual path, but depends mostly on the final state.[6] For a given value of K_L, we also varied K and G to ensure that the results were not sensitive to small variations in these values.

Table I. Electromechanical Constants of Ytterbium Foils

Physical Property	Value
Bulk Modulus[a]	148 kb
Young's Modulus	163 kb
Yield Stress in Simple Tension	0.78 kb
Strain Hardening Coefficient, M^b	7.12 kb
Piezoresistive Coefficient, $\pi_{11}{}^b$	$-4.196 \times 10^{-2}(\text{kb})^{-1}$
Piezoresistive Coefficient, $\pi_{12}{}^b$	$-0.787 \times 10^{-2}(\text{kb})^{-1}$
Electrical Strain Hardening Coefficient, η^b	1.08 kb

[a] From Grady and Ginsberg (Ref. 9).
[b] Defined in Reference 4.

Table II. Summary of the results from dynamic experiments.

Experiment Number	Projectile Velocity (mm/μsec)	Matrix Longitudinal Stress (kbars)	Gauge G1		Gauge G2	
			$(\Delta R/R_0)_{peak}$	$(\Delta R/R_0)_{res.}$	$(\Delta R/R_0)_{peak}$	$(\Delta R/R_0)_{res}$
1. (85534)[a]	0.098	2.8	0.14	0.016	0.12	0.015
2. (85522)	0.149	9.4	0.68	0.11	0.66	0.075
3. (85530)	0.247	15.2	1.38	0.10	1.36	0.099
4. (85547)	0.330	20.0	1.95	0.12	1.95	0.12
5. (85548)	0.414	25.0	2.66	0.14	2.57	0.13
6. (85576)[b]	0.507	30.0	3.54	--	--	--
7. (85577)[b]	0.596	35.0	3.97	--	--	--
8. (85580)[c]	0.597	35.1	--	--	4.02	--
9. (85582)[c]	0.679	39.6	--	--	4.17	0.182

[a] This experiment had a PMMA impactor; the remaining experiments had fused silica impactors.

[b] Data from guage G2 were very noisy.

[c] These experiments had only one guage G2 in the target.

Table III. Measured and calculated residual resistance charge

Peak Longitudinal Stress (kbar)	$\Delta R/R_0$ (Measured)	$\Delta R/R_0$ (Calculated)		
		Due to Residual Stresses and Strains	Due to Plastic Deformation	Total
2.8	0.015	0.035	0.001	0.036
9.4	0.092	0.062	0.015	0.077
15.2	0.099	0.078	0.021	0.098
20.0	0.120	0.091	0.027	0.118
25.0	0.135	0.104	0.028	0.132
39.6	0.182	0.151	0.033	0.184

FIGURE CAPTIONS

1. Schematic view of the flyer and the target assembly.

2. Typical resistance change ($\Delta R/R_o$) versus time profile measured in our experiments. This record is for gauge G1 at a matrix stress of 25 kbar.

3. Resistance change ($\Delta R/R_o$) versus time profiles for ytterbium and manganin gauges in the experiment at a matrix stress of 45 kbar. The resistance change scale for the manganin gauge is shown on the right side of the Figure.

4. Calculated and measured values of $(\Delta R/R_o)_{peak}$ as a function of peak longitudinal stress in the matrix.

5. Calculated and measured values of $(\Delta R/R_o)_{residual}$ as a function of peak longitudinal stress in the fused silica matrix. For comparison, results for the PMMA matrix from Ref. 5 are also shown. The broken line through the PMMA data is a smooth curve drawn to fit the data and does not represent calculated values.

6. Measured $(\Delta R/R_o)_{peak}$ as a function of peak longitudinal matrix stress in fused silica and in PMMA. The lines are smooth curves drawn to fit the data and do not represent calculated values.

FLYER
FUSED SILICA

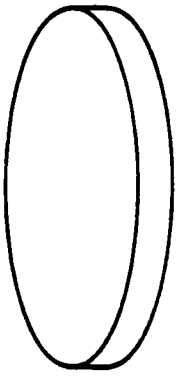

3.17mm

TARGET ASSEMBLY
FUSED SILICA

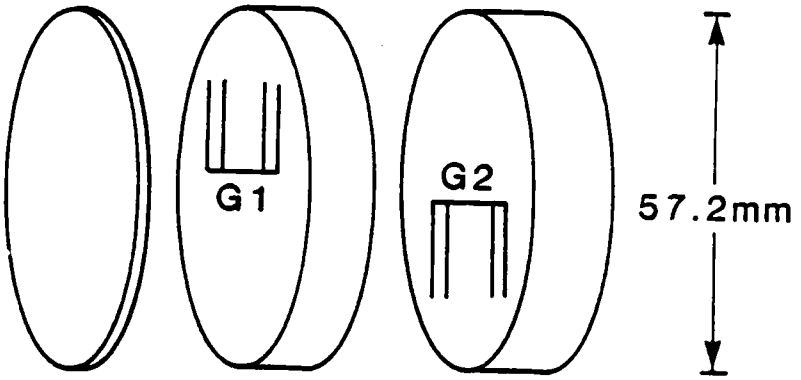

1.0mm 6.35mm 9.52mm

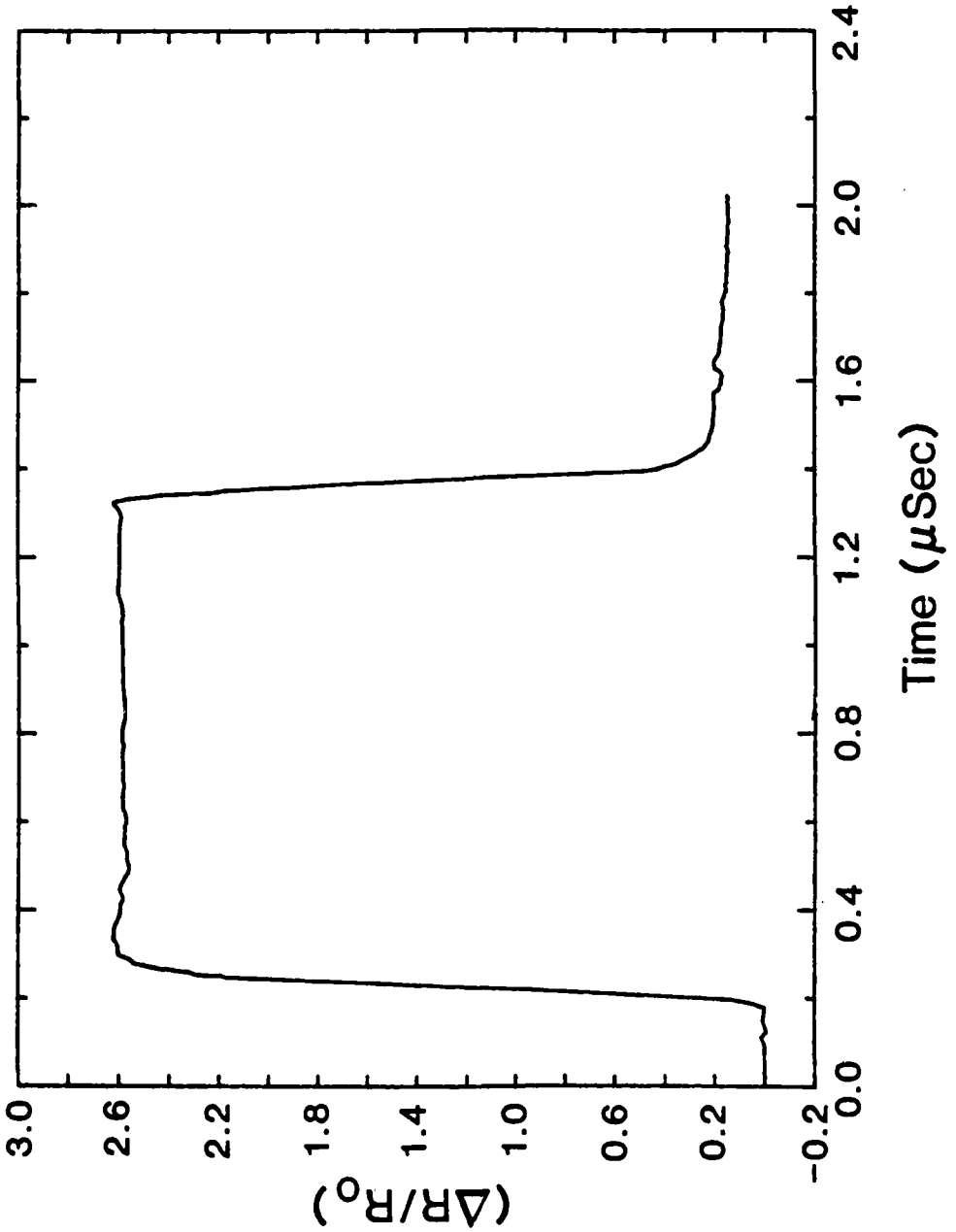
3.0
2.6
2.2
1.8
1.4
1.0
0.6
0.2
−0.2
0.0
0.4
0.8
1.2
1.6
2.0
2.4
(ΔR/R$_o$)
Time (μSec)

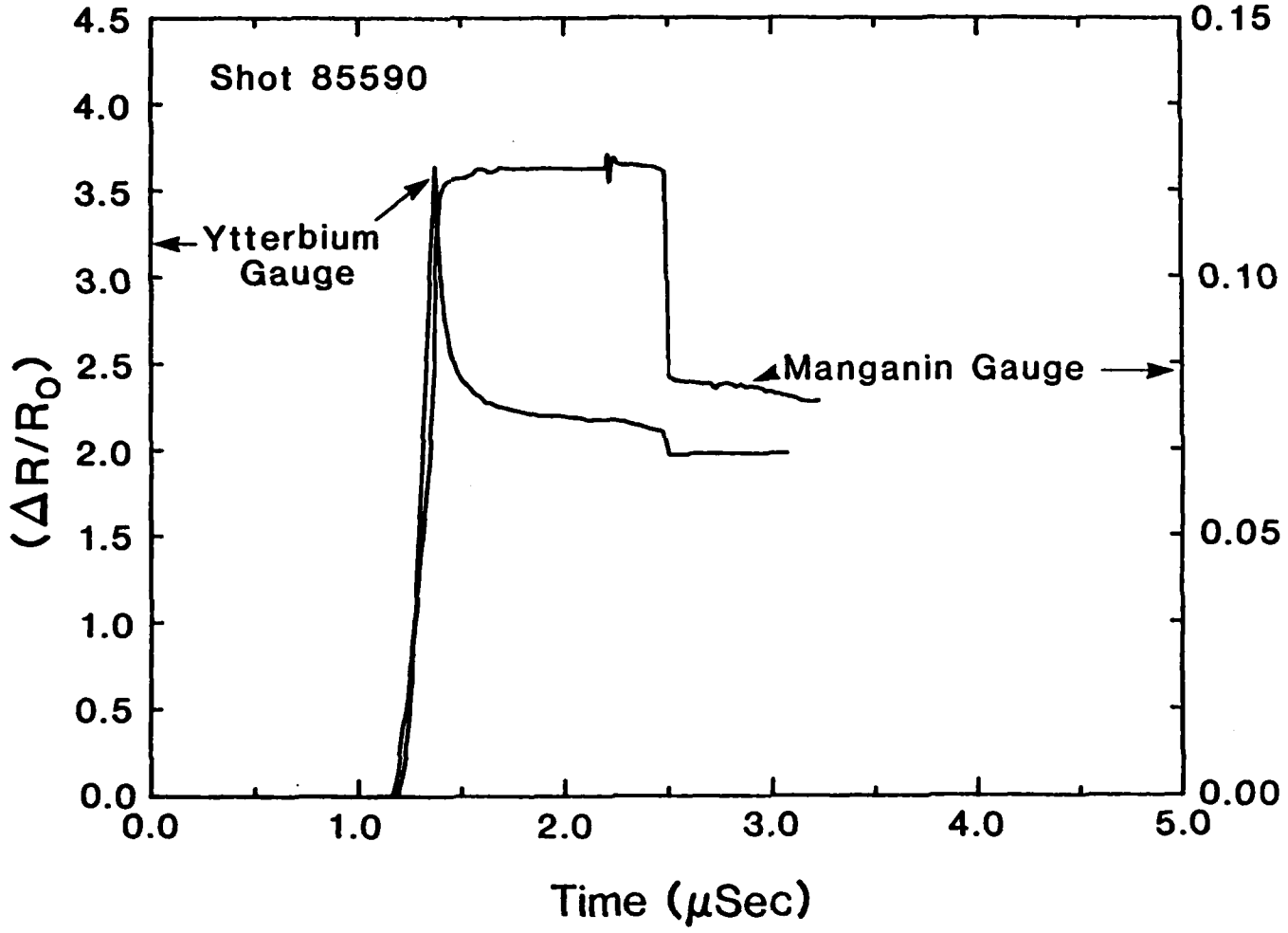
Shot 85590
Ytterbium Gauge
Manganin Gauge
$(\Delta R/R_o)$
Time (μSec)
4.5
4.0
3.5
3.0
2.5
2.0
1.5
1.0
0.5
0.0
0.15
0.10
0.05
0.00
0.0
1.0
2.0
3.0
4.0
5.0

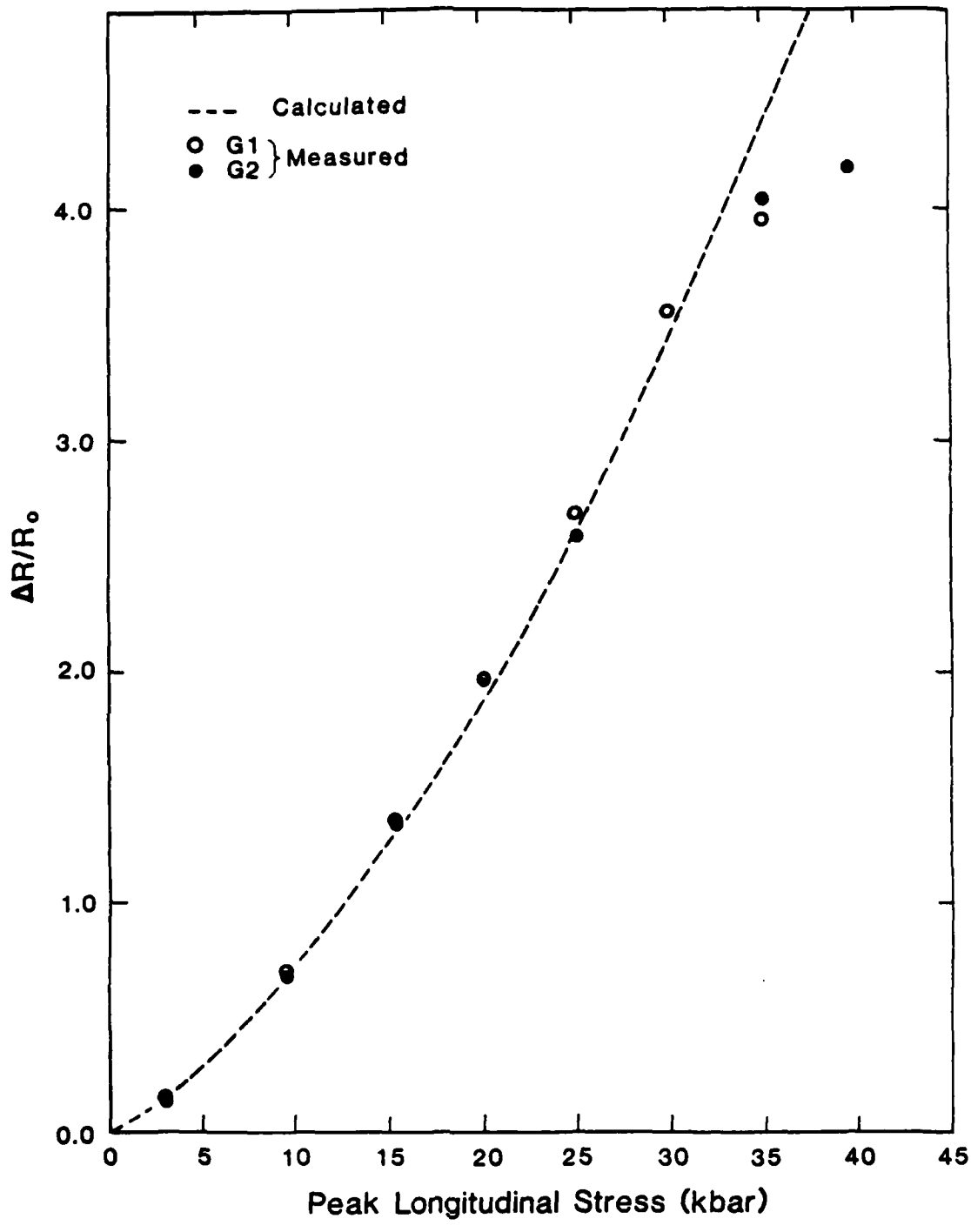
Calculated
G1
G2
Measured
4.0
3.0
2.0
1.0
0.0
ΔR/R₀
0
5
10
15
20
25
30
35
40
45
Peak Longitudinal Stress (kbar)

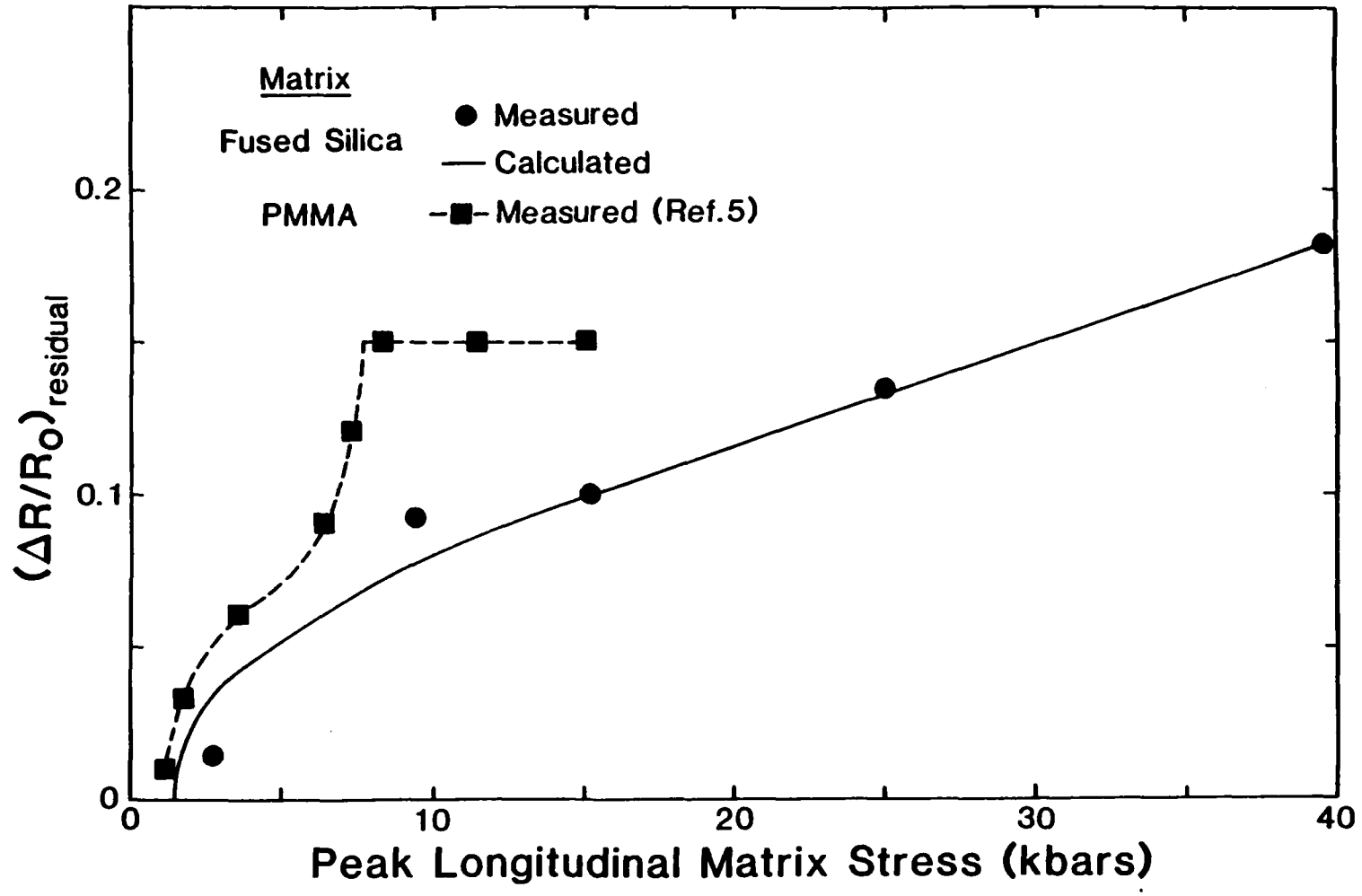
Matrix
Fused Silica
PMMA
Measured
Calculated
Measured (Ref.5)
$(\Delta R/R_o)_{residual}$
0.2
0.1
0
0
10
20
30
40
Peak Longitudinal Matrix Stress (kbars)

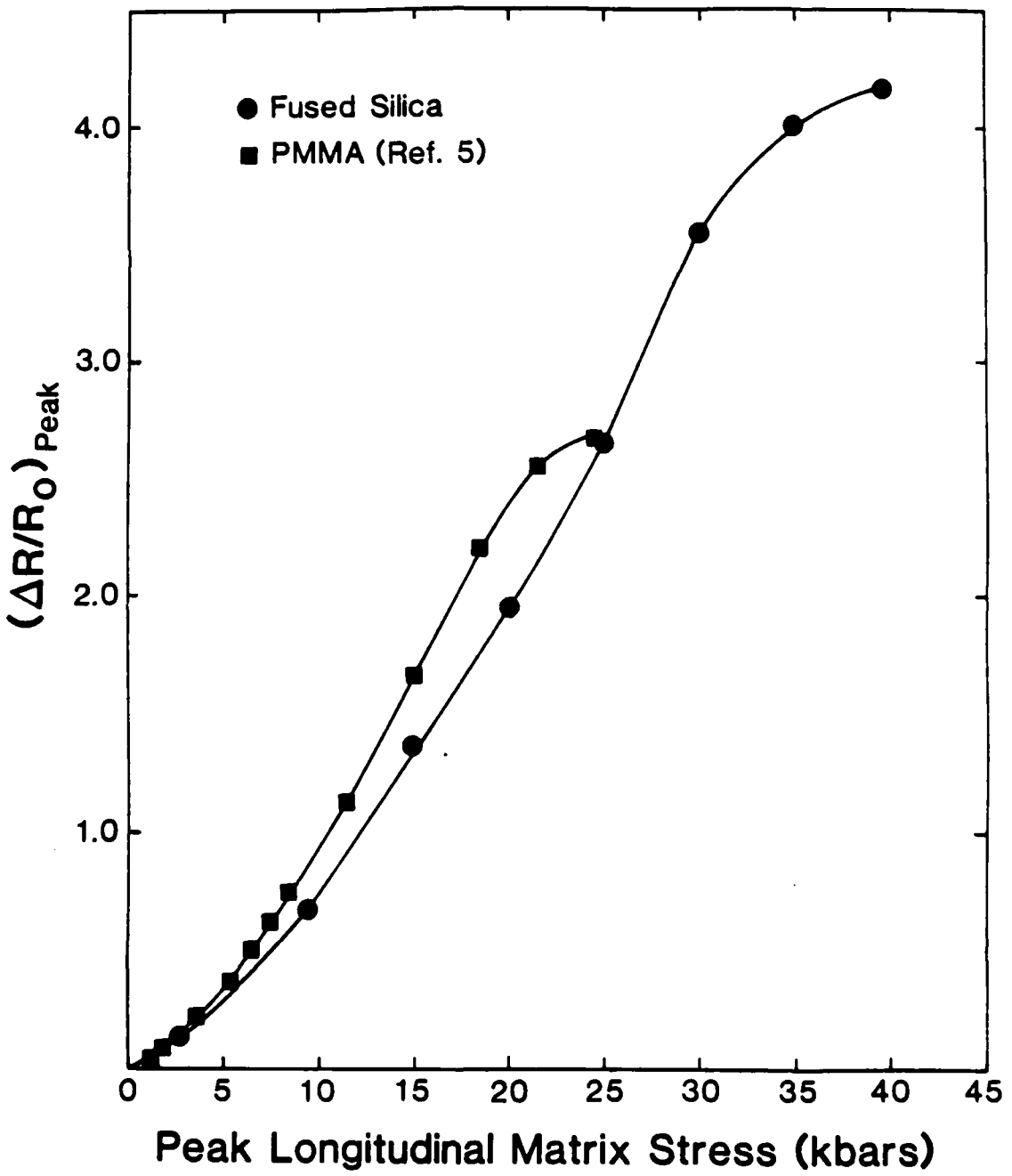
Fused Silica
PMMA (Ref. 5)
4.0
3.0
2.0
1.0
$(\Delta R/R_o)_{Peak}$
0
5
10
15
20
25
30
35
40
45
Peak Longitudinal Matrix Stress (kbars)

END

12-86

DTIC